UNIVERSITY OF OKLAHOMA

GRADUATE COLLEGE

PERFORMANCE OF FIBER-REINFORCED SELF-CONSOLIDATING CONCRETE FOR REPAIR OF BRIDGE SUB-STRUCTURES

A THESIS

SUBMITTED TO THE GRADUATE FACULTY

in partial fulfillment of the requirements for the

Degree of

MASTER OF SCIENCE

By

COREY WIRKMAN
Norman, Oklahoma
2016

PERFORMANCE OF FIBER-REINFORCED SELF-CONSOLIDATING CONCRETE FOR REPAIR OF BRIDGE SUB-STRUCTURES

A THESIS APPROVED FOR THE
SCHOOL OF CIVIL ENGINEERING AND ENVIRONMENTAL SCIENCE

BY

_____
Dr. Jeffery Volz, Chair

_____
Dr. Chris Ramseyer

_____
Dr. Royce Floyd

ACKNOWLEDGEMENTS

First, I would like to thank my advisor and mentor, Dr. Jeffery Volz, for helping me though this long and challenging process, and above all for making graduate school a worthwhile and memorable experience. His knowledge, guidance, and most importantly his kindness helped make my graduate career as rewarding and enjoyable as possible.

I would like to thank the Oklahoma Department of Transportation and Dolese Brothers for the funding support that they provided for this project, as well as the University of Oklahoma for the financial support that allowed me to focus on my studies.

I would also like to thank my committee members, Dr. Chris Ramseyer and Dr. Royce Floyd for their time and advice in reviewing this thesis and making suggestions for improvement.

I would like to thank our lab technician Michael Schmitz, whose invaluable knowledge and experience made all of our projects that much easier. I owe many thanks to my fellow graduate and undergraduate students Jon Drury, Derek Garcia, Jacob Choate, Austin Messerli, Kodi Wallace, Hesham Tuwair, Alixandra Bradford, Mason Moore, and Nischal Pradhan for their invaluable support in constructing and testing my specimens.

Finally, I would like to thank my family for always supporting me throughout both my undergraduate and graduate career and for letting me know that they are always there for me.

TABLE OF CONTENTS

LIST OF TABLES

LIST OF FIGURES

ABSTRACT

The damage of various reinforced concrete elements accounts for significant annual expenditures by state and federal transportation agencies on bridge maintenance, repair, or replacement. With the rising costs of materials and labor, as well as a demand for faster construction, the development of cheaper and faster alternatives has become a necessity. Concrete types, such as fiber-reinforced self-consolidating concrete (FR-SCC), make large strides towards making these new construction demands a possibility. FR-SCC, for instance, is a high performance concrete characterized by its ability to flow under its own weight eliminating the need for vibration, cutting down on labor costs and speeding up construction while also having improved tensile performance in the hardened state.

The main objective of this study was to investigate key engineering and structural properties of bridge substructures retrofitted with fiber-reinforced self-consolidating concrete tension zones. The testing program compared FR-SCC repair mix designs at two different Komponent, a Type-K shrinkage-compensating cement, replacement levels: 10% replacement, denoted as C-10%, and 15% replacement, denoted as C-15%. A standard Oklahoma Department of Transportation (ODOT) Class AA mix was used as a baseline control mix throughout the study. In addition to material properties testing, both small-scale and full-scale repair tests were conducted. The small-scale repair tests included Third Point Loading Composite Prism Tests as well as Bond Strength Tests. The

full-scale tests included a total of 9 beam specimens. One set of 3 control beams (C-C), and two sets of 3 repair beams representing either C-10% or C-15%. While the small-scale tests provided a good indicator on how the two concretes were going to interact, the full-scale beams allowed for a more realistic stress state response in evaluating the flexural performance of these repairs.

Overall, the two repair concretes, C-10% and C-15%, examined throughout this study showed comparable load-carrying capacities and cracking loads to the monolithic control beams. In addition, analysis of the fresh concrete material properties indicated that highly workable FR-SCC can be made using synthetic fibers and local materials. The investigated mixtures fulfilled all the passing ability, filling capacity, and stability requirements needed to provide a successful repair. Analysis of the small-scale test results indicated that both C-10% and C-15% fiber-reinforced self-consolidating repair concretes performed comparably to the control ODOT Class AA concrete. In addition, the two sets of FR-SCC repair beams were statistically equivalent to the control beams. They had similar ultimate moments, almost identical load versus deflection plots, and had relatively similar cracking behaviors.

1. INTRODUCTION

1.1 BACKGROUND AND JUSTIFICATION

Damage of reinforced concrete elements accounts for significant annual expenditures by state and federal transportation agencies on bridge maintenance, repair, or replacement. While new bridges are designed to function for 75 to 100 years, they will require substantially more long-term attention and service support. Because of the limited infrastructure budget, an increased service life is also being expected out of infrastructure repair sections. In the coming years, maintenance and construction costs associated with infrastructure throughout the country will continue to increase faster than available matching funds. A recent survey by the United States Department of Transportation classified roughly 27.5 percent of the nearly 600,000 bridges with spans over 20 feet as "structurally deficient" and noted that "preservation strategies will become paramount" as funding continues to shrink (USDOT, 2014). According to the Turner Fairbank Highway Research Center, there is about 2.3 billion square feet of bridge-deck surface associated with the federal highway system. For each year that the lifetime of a bridge is extended, approximately $8 per square foot will be saved (Kassimi, 2014).

The rising costs of materials and labor, as well as the demand for faster construction, has prompted development of cheaper, faster alternatives to conventional building techniques. Self-consolidating concrete (SCC) is a high performance concrete characterized by its ability to flow without segregation

under its own weight. In addition, eliminating vibration cuts down on the labor needed and speeds up construction. This increase in speed results in faster placement rates, cost savings, and fewer traffic disruptions. The reduction of equipment usage also lessens wear and tear and noise levels in both concrete plants and at construction sites, improving jobsite safety. Furthermore, lack of vibration reduces aggregate segregation, honeycombing, and voids in the concrete. In repair applications, SCC has proved to be advantageous in facilitating the repair operations, including hard-to-reach areas and congested sections. Many of these applications can be found in bridge substructures (piers, girders, pile caps, abutments, etc.).

The first documented case study involving the use of SCC in repair operations involved the rehabilitation of a parking garage in downtown Sherbrooke, Quebec, in 1996. SCC was used for the repair of the bottom and vertical sides of a 20 foot long beam exhibiting advanced corrosion damage situated under an expansion joint at the entrance to the parking structure. The repair section contained longitudinal reinforcing bars and stirrups anchored into the existing concrete that presented serious obstacles for the spread of fresh concrete. The concrete was cast from two 4-inch diameter holes drilled from the upper deck of the beam along the outer length of the beam between the existing concrete and formwork. The developed SCC mix was shown to flow under its own weight along the highly restricted section and around the vertical side to fill the opposite side of the formwork through narrow spacing. Due to its success, the

Quebec Department of Transportation developed its first performance-based specifications for SCC in 1997 and has used SCC in several infrastructure rehabilitation projects. Experience with SCC has shown that in addition to its ease of casting characteristics, the concrete can exhibit high durability and good bond to existing surfaces and reinforcement (Kassimi, 2014).

Successful experience with the performance of SCC as a superior repair material has attracted the attention of construction firms and departments of transportation. Examples of the repair of damaged bridge substructures are given in Figures 1.1 thru 1.3.

Figure 1.1 SCC Used in the Repair of Bridge Pier Caps

Figure 1.2 SCC Used in the Repair of Bridge Piles

Figure 1.3 SCC Used in the Repair of Bridge Columns and Pier Caps

As in other repair applications, repair sections made with concrete are prone to cracking due to restrained shrinkage. Recently, fiber reinforcement has been used in SCC to control cracking and increase tensile and flexural strength. Fiber reinforced self-consolidating concrete (FR-SCC) combines the benefits of SCC in the fresh state with improved performance in the hardened state. One of the earliest uses of FR-SCC was in the Jarry/Querbes Underpass in Montreal. The structure had undergone severe degradation due to aggressive exposure to frost action. The project was successfully repaired with the use of FR-SCC. The use of synthetic structural fibers was beneficial in obtaining only small and finely distributed surface cracking. This project is shown in Figure 1.4 below.

Figure 1.4 FR-SCC in the Repair of Jarry/Querbes Underpass

The performance of FR-SCC depends on the type of fibers in use. Several fiber types exist on the market, and they should be selected wisely to secure the

intended objectives. Kassimi and Khayat recently carried out an extensive investigation to evaluate the performance of various fibers in SCC targeted for repair applications (Kassimi, 2014). The concrete mixtures were tested for workability, mechanical properties, drying and restrained shrinkage, flexural creep, and some structural behavior in flexure. Polypropylene fibers, a hybrid of steel and polypropylene, and steel fibers were used. Although limited in scope, the investigation revealed that the incorporation of fibers along with an expansive agent (EA) can enhance the resistance to restrained shrinkage. The improvement was greater than that observed in FR-SCC without EA or that for SCC with EA. In addition, a synergetic effect was observed where the presence of fibers and EA secured superior resistance to cracking in concrete. This is a key requirement to enhance the service life of a repair.

1.2 OBJECTIVES AND SCOPE OF WORK

The main objective of this study was to investigate key engineering and structural properties of FR-SCC in infrastructure repair and construction utilizing local materials and labor. The expected result of this study was to discover the effects of varying levels of expansive agent replacement, specifically Komponent, a Type-K shrinkage-compensating cement. This experimental study consisted of comparing the structural performance of two FR-SCC mixes designed at different Komponent replacement levels to an Oklahoma Department of Transportation (ODOT) standard Class AA mix design. Additionally, the

study compared the structural performance of repaired beam elements, using these FR-SCC mixes for the repair of the tension zone, to a set of monolithic control beams made from the ODOT Class AA mix.

The following scope of work was implemented in an effort to reach this objective: (1) review the applicable literature; (2) develop a research plan; (3) develop control and FR-SCC mix designs; (4) design and construct test fixtures; (5) design and construct test specimens; (6) test specimens to failure and record the applicable data; (7) analyze the results and conduct comparisons between the two FR-SCC repair mixes and the control mix designs; (8) develop conclusions and recommendations; (9) prepare this thesis in order to document the information obtained during this study.

1.3 RESEARCH PLAN

For this experimental program, the structural performance in the repair of bridge substructures of two FR-SCC mix designs at different Komponent replacement levels was investigated and compared with a standard ODOT mix design. The Komponent mix design procedure investigated was the direct replacement method. This design method is a volumetric procedure that replaces a percentage of the cement content directly with Komponent. For this study, the two replacement levels that considered were 10% and 15%.

To investigate the structural performance of the FR-SCC in the repair of bridge substructures, both small-scale and full-scale composite tests were

performed in addition to the standard material property tests. The small-scale tests included Third Point Loading Composite prism tests based on ASTM C 78 *Standard Test Method for Flexural Strength of Concrete,* as well as Bond Strength Tests based on ASTM C 882 *Standard Test Method for Bond Strength of Epoxy-Resin Systems Used With Concrete By Slant Shear.* The full-scale tests consisted of a total of 9 beam specimens. One set of 3 monolithic control beams constructed with the ODOT Class AA control mix, and two sets of 3 repaired beams utilizing the two FR-SCC mix designs to repair the tension zones.

1.4 OUTLINE

This thesis consists of six chapters and two appendices. Chapter 1 contains a brief explanation of the history, current uses, and benefits of FR-SCC as well as the objective and scope of work of this study. Chapter 2 provides an overall discussion of the literature on the benefits and properties of FR-SCC, the mix design and methodology for developing fiber-reinforced concrete, and the properties of fiber-reinforced concrete.

Chapter 3 details the mix designs that were developed for this study as well as the test methods used to determine fresh and hardened concrete properties. Chapter 4 then discusses the design, fabrication, test set-up, and test procedure for the full-scale beam specimens.

Chapter 5 begins the evaluation and analysis of the tests conducted in the previous chapters. It also provides the test methods used to determine the

hardened concrete properties of the composite specimens, the recorded test data, and a comparison of the structural performance of the two Komponent replacement levels with the control specimens. Chapter 6 then summarizes the findings, conclusions, and recommendations from this study. Finally, the appendices include the complete structural performance data from each of the full-scale tests and photographs from the full-scale tests.

2. LITERATURE REVIEW

2.1 INTRODUCTION

In order to fully understand the current knowledge on which we are trying to expand for FR-SCC as used in repair sections, a comprehensive literature review of previous experiences and research findings on its design and use must be completed. A detailed study about the mix design and methodology of fiber-reinforced concrete and special workability test methods that can be used for FR-SCC will be reviewed. Utilizing these articles, various research needs will be identified in order to help answer these important issues.

The literature review will also focus on studies involving the hardened properties of SCC and fiber-reinforced concrete, including mechanical properties (compressive strength, flexural strength, fracture energy, and cracking resistance), structural properties (bond, shear, and flexural strengths), and durability (freeze-thaw resistance, permeability, and electrical resistivity). Special attention will be given to fiber orientation in FR-SCC and its effect on mechanical performance and cracking resistance.

2.2 FR-SCC BENEFITS AND PROPERTIES

According to Holt (2004), one of the biggest technological advancements that can be made in concrete formulation is the reduction of time and labor requirements while still providing a strong and durable material. Self-consolidating concrete (SCC) is a relatively new category of high-performance

concrete that exhibits a "low resistance to flow to insure high flowability." Figure 2.1 summarizes the basic workability requirements for a generally successful casting of SCC (Khayat, 1999b).

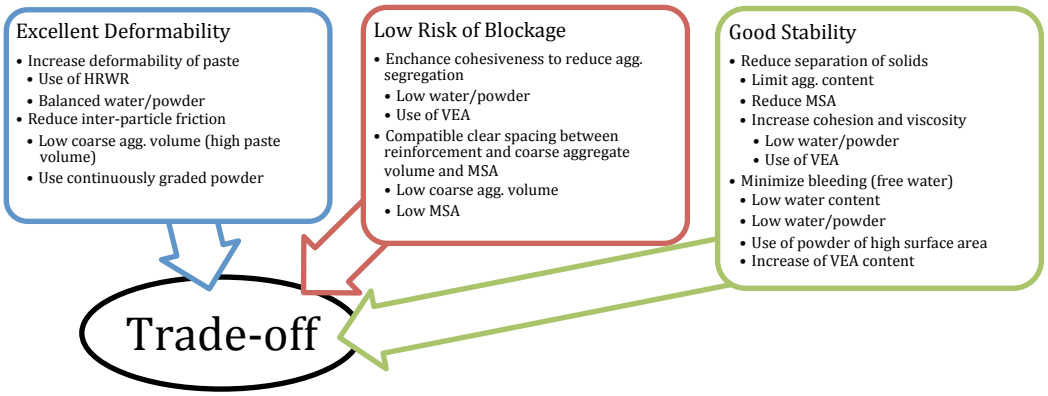

Figure 2.1 Basic Workability Requirements for SCC

In addition to these general requirements, the required workability for casting concrete also depends on the type of construction, selected placement and consolidation methods, the complex shape of the formwork, and structural design details that affect the reinforcement congestion. The use of SCC has been widespread in Japan since the late 1980s for casting congested members, as well as the placement of concrete in restricted areas where consolidation may not be practical such as the repair of beams, girders, and slabs (Khayat, 1999b). The addition of discrete fibers to SCC with adequate mechanical properties can therefore significantly improve many of the engineering properties of the concrete, most notably impact strength and toughness. "Flexural strength, fatigue strength, and the ability to resist cracking and spalling are also enhanced" (Kassimi, 2014).

2.3 MIX DESIGN AND METHODOLOGY OF FR-SCC

The mix design of SCC requires "careful tailoring of mixture constituents to secure a proper balance between contradictory properties necessary for the successful production of such a complex material" (Khayat, 1999a). These contradictory properties are workability (or flowability) and strength. Figure 2.2 illustrates the trade-off between these two characteristics, with strength represented by the stability of the concrete. Higher stability in this case leads to a better chance for particle dispersion and deformability, and in turn compressive strength.

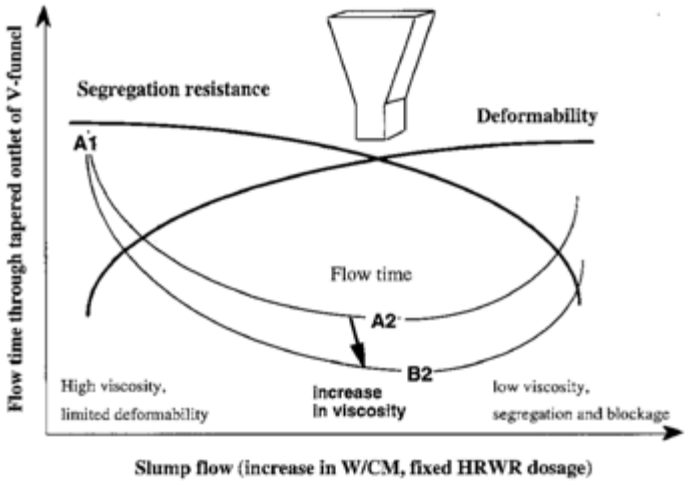

Figure 2.2 Trade-off Between Workability and Stability

Flowability is primarily affected by inter particle friction that increases in the vicinity of obstacles due to greater collision rates. This friction and these collisions lead to greater viscosity and an increased need for vibration techniques to help keep the concrete flowing (Khayat, 1999a). Because of this, SCC has a higher portion of fine contents, including sand, cementitious materials, and

chemical admixtures that help reduce friction and therefore particle collisions (Holt, 2004). In 1999, Khayat, Ghezal, and Hadriche developed a widely available series of statistical models that can simplify the test protocol required to optimize a given mixture. This simplification leads to a reduction of the number of trial batches needed, as well as a factorial design approach which provides an efficient means to determine the key variables of SCC mix designs (Khayat, 1999a).

Early in 2014, Kassimi et al. concluded that the proper use of a high volume of fiber reinforcement in SCC is "challenging given the hindering effect of fibers on SCC characteristics" (Kassimi, 2014). Because of this, a study trying to derive the optimal fiber reinforcement volume while still maintaining optimal flowability, passability, and stability was started. Through experimental investigations it was derived that high flowability can still be obtained when the volume of fibers is limited to 0.5%. This allowed for proper fiber alignments and flow while still creating a repair material that was sufficiently strong to allow a beam to perform at maximum capacity. A fiber volume larger than this started to reduce the flowability of the concrete, creating adverse effects on both strength and segregation (Kassimi, 2014).

2.4 PROPERTIES OF FR-SCC

Fibers are made of different materials and geometrics that lead to improvements of different concrete properties. For example, "steel fibers are

incorporated to enhance mechanical properties, whereas polypropylene fibers are mainly used to reduce cracking due to plastic shrinkage" (Kassimi, 2014). In order for FR-SCC to be used in repair, the correct type of fiber must be chosen in order to create a "good repair." In general, a "good repair" improves the function and performance of a structure restoring or increasing its initial strength and stiffness while enhancing the appearance of the concrete surface and its durability. During a study on FR-SCC used in repair beam elements, Kassimi was able to derive that FR-SCC made using steel, synthetic, or hybrid fibers incorporated at a volume of up to 0.5% created suitable repairs for many beam applications. It was derived that fibers were able to flow horizontally under their own weight and were able to achieve good compaction in the absence of vibration (Kassimi, 2014).

2.5 FULL-SCALE TESTING OF FR-SCC

While there are several studies on the development of FR-SCC mix designs, there is limited literature related to the structural use of FR-SCC in beams, especially in the repair of beam substructures. Cohen (2008) performed a study on FR-SCC used in the construction of monolithic beam sections for both flexural and shear tests. He noted that the addition of fibers to a SCC mix improved the shear capacity of the beam while also altering the brittle shear failure mode allowing for a more ductile flexural response in shear-critical beams. Cohen also noted that the addition of the fibers led to an improvement in

cracking behavior, which was shown through better control of crack widths and a reduction in crack spacing.

Kassimi (2013) expanded on this idea and others and used it in the repair of bridge substructures, in which the effective tension zone was repaired given either advanced cracking or advanced corrosion of the bottom steel reinforcement. He found that the additional shear capacity provided by the fibers helped prevent shear cracks from starting, even in areas where the bond to the existing shear reinforcement was not fully developed.

Expanding on his previous research, Kassimi et al. (2014) looked further into the effects of various fibers and amounts in these repair applications. The authors noted that "the beams repaired with the various self-consolidating mixtures made with fibers showed comparable load-carrying capacities and higher cracking loads than the reference monolithic beam." They also noted that beams repaired with steel or long multifilament polypropylene fibers exhibited better structural performance in terms of load-carrying capacity and cracking resistance than those repaired with monofilament polypropylene or hybrid fibers.

Kassimi (2013) noted, however, that the addition of shrinkage-reducing agents, such as Komponent, could lead to considerable overall improvement. The addition of the expansive agent could reduce drying shrinkage as well as better dimensional stability and less stress at the bond interface (Emmons, 1993). Therefore, the addition of Komponent is the next step that this thesis will be taking to help further develop FR-SCC as a bridge substructure repair material.

3. MIX DESIGN AND CONCRETE PROPERTIES

3.1 INTRODUCTION

The following section discusses the procedures used to determine the fresh as well as hardened properties of the three mix designs used in this study. A detailed outline of the mix designs developed and their respective properties is also discussed in this section.

3.2 CONCRETE PROPERTIES

3.2.1 Fresh Concrete Properties

For the three mixes used in this study, the fresh concrete property tests that were performed were slump, unit weight, air content, as well as an initial flow test for the FR-SCC. The slump test for the control concrete was performed in accordance with ASTM C 143 *Standard Test Methods for Slump of Hydraulic Cement Concrete.* The inside of a standard slump cone was wetted and placed on a damp slump flow board. For the control concrete, concrete was added to the cone in three equal lifts and rodded 25 times each lift with the appropriately dimensioned steel rod. In accordance with ASTM C 1611 *Standard Test Method for Slump Flow of Self-Consolidating Concrete,* the FR-SCC concrete was added in one full lift and was not rodded. Concrete was then struck off at the top of the cone using the rod, and any extra concrete was removed from around the base of the cone. The cone was lifted at a constant rate over five seconds. For the control concrete, the cone was inverted next to the slumped concrete and the slump

measurement was taken from the rod placed over the top of the inverted cone to the center of the slumped concrete. For the FR-SCC concrete, the cone was set aside and the slump flow was measured as the average of two perpendicular diameters of the concrete flow.

The unit weight of the concrete was determined in accordance with ASTM C 138 *Standard Test Method for Density (Unit Weight), Yield, and Air Content (Gravimetric) of Concrete.* For the control concrete, a steel measure of known volume was weighed and then filled with concrete in three equal lifts. Each lift was rodded 25 times and tapped with a rubber mallet to help consolidate the concrete. For the FR-SCC, a similar steel measure of known volume was weighed and then filled with concrete in one full lift. The lift was not rodded but was tapped with a rubber mallet to help consolidate the concrete. Once filled, a steel plate was used to screed the top surface of the measure to remove the excess concrete and create a smooth and level surface. A wet sponge was used to wipe away excess concrete from the outside of the measure and along the top rim. The measure was then weighed, and the unit weight was determined.

The air content of the fresh concrete was determined in accordance with ASTM C 231 *Standard Test Method for Air Content of Freshly Mixed Concrete by the Pressure Method* using a Type B pressure meter. After the unit weight was determined, the same measure filled with concrete was used to determine air content. The pressure meter lid was wetted and secured over the top of the measure. The air chamber on the top of the lid was sealed off, and the appropriate

initial pressure was added to the chamber. Next, water was injected into one petcock until it flowed without air bubbles from the opposite petcock ensuring the space between the lid and the surface of the concrete was filled with water. The petcocks were then closed, and the air from the chamber was injected into the concrete-filled bottom measure while simultaneously tapping the measure with a rubber mallet. The air content was then recorded from the gauge on the pressure meter.

The initial flow test for the FR-SCC was used to determine if the mix could flow under its own weight the entire length of a 14 ft.-long beam while also reaching the repair depth of 6 in. throughout. On one side of the beam mold was a 4 in.-diameter, PVC pipe set-up as shown in Figure 3.1, which represented the fill hole that would later be created in the control concrete in order to repair the beam. The concrete was then funneled into the PVC pipe via a concrete bucket and large funnel (Figure 3.2). While pouring into the funnel, the opposite side was monitored to see if the concrete reached a minimum depth of 6 in., marked with a grease pencil on the side of the beam form.

Figure 3.1 Flow Test Fill Hole Set-Up

Figure 3.2 Flow Test SCC Pour

3.2.2 Compressive Strength of Concrete

The compressive strength, f'_c, of the concrete was determined as per ASTM C 39 *Standard Test Method for Compressive Strength of Cylindrical Concrete Specimens.* For each set of beam specimens and repairs, accompanying cylinders were made to determine the compressive strength. For the control concrete, the cylinder molds had a diameter of 4 in. and a height of 8 in. For the FR-SCC, the cylinder molds had a diameter of 6 in. and a height of 12 in. due to the 2.1 in.-long fibers used in each mix. All the cylinders were left to cure in the same condition as the beam specimens described later. The compressive strength of the concrete was tested at 1, 3, 7, 21, and 28 days as well as on the days of testing the beam specimens. Prior to testing, the cylinders were ground down with the Marui Concrete Specimen End Grinder to give a uniform stress distribution during testing. The cylinders were loaded between 28 psi/sec and 42 psi/sec as per the ASTM C 39 standard. Figures 3.3 and 3.4 show a ground 4 in.

x 8 in. cylinder and a 6 in. x 12 in. cylinder, respectively, in the loading machine. Three specimens were tested with the average representing one compressive strength data point. The compressive strength of each mix design was determined from these companion cylinders on the day of testing.

Figure 3.3 4x8 Compression Cylinder Test Set-Up

Figure 3.4 6x12 Compression Cylinder Test Set-Up

3.2.3 Modulus of Rupture of Concrete

The modulus of rupture, f_r, was determined as per ASTM C 78 *Standard Test Method for Flexural Strength of Concrete.* Small beams with dimensions of 6 in. x 6 in. x 20 in. or 6 in. x 6in. x 21 in. were cast to find the modulus of rupture. To test these beams, simple third point loading was used with a span length of 18 in as shown in Figure 3.5. Upon reaching the peak load of the test, the modulus of rupture was calculated by Equation 3.1:

$$f_r = \frac{P*L}{b*d^2} \qquad \text{(Eq. 3.1)}$$

where P is the peak load, L is the beam span, and b and d are the beam width and depth, respectively, measured at the fractured surface of the beam. Three specimens were tested with the average representing one strength data point.

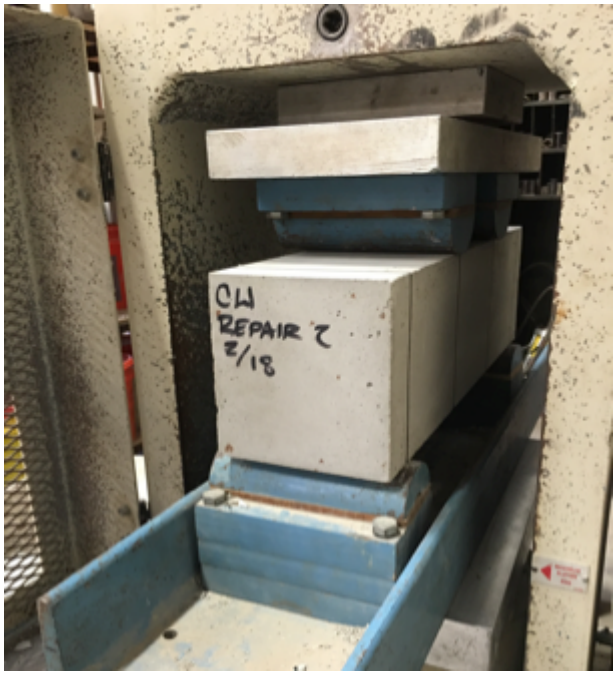

Figure 3.5 Modulus of Rupture Test Set-Up

3.2.4 Modulus of Elasticity of Concrete

The modulus of elasticity, E_c, of the concrete was determined in accordance with ASTM C 469 *Standard Test Method for Static Modulus of Elasticity and Poisson's Ratio of Concrete in Compression.* For the control concrete, cylinders with a 4 in. diameter and 8 in. height were used to determine modulus of elasticity. For the FR-SCC concrete, cylinders with a 6 in. diameter and 12 in. height were used. The modulus of elasticity for each mix design was determined from companion cylinders to the beam specimens at the standard 28-day mark.

3.2.5 Splitting Tensile Strength of Concrete

The splitting tensile strength, f_{tsp}, of the concrete was determined as per ASTM C 496 *Standard Test Method for Splitting Tensile Strength of Cylindrical Concrete Specimens.* For the control concrete, 4 in. x 8 in. cylinders were used, while 6 in. x 12 in. cylinders were used for the FR-SCC. Three specimens were tested at the 28-day mark as shown in Figure 3.6. Upon reaching the peak load of this test, the splitting tensile strength was found by Equation 3.2:

$$f_{tsp} = \frac{2*P}{\pi*L*D} \qquad \text{(Eq. 3.2)}$$

where P is the peak load, L is the cylinder length, and D is the cylinder diameter. The average of these three values was then used to represent one splitting tensile strength data point. The splitting tensile strength of each mix design was determined from companion cylinders to the beam specimens.

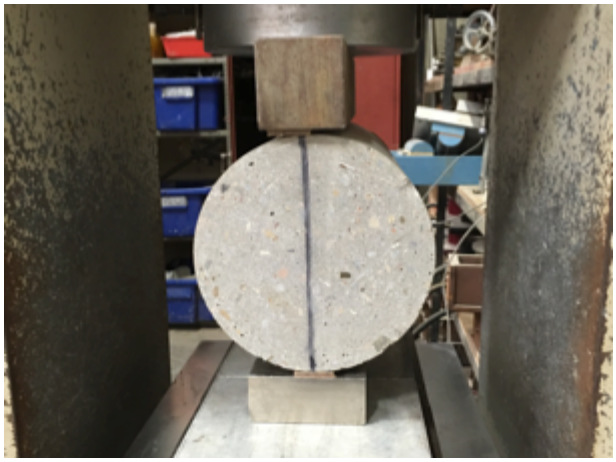

Figure 3.6 Splitting Tensile Test Set-Up

3.3 CONTROL AND FR-SCC MIX DESIGNS

In this study, three mix designs were developed and evaluated for flexural performance in either a monolithic beam configuration or a composite repair beam. An ODOT Class AA mix design was used as a baseline reference and control concrete throughout the study. The specified cement content in this mix was 588 lb., the Class F Fly Ash replacement was 20% by mass, the water-to-cement ratio was 0.40, the target slump was 3 in., and the design air content was 6%. The specified amount of fine aggregate as a volume of total aggregates was 40%. As per specifications, this mix called for the typical dosage range of ODOT-approved air entertainer MB-AE 90 (0.25-4.0 fl. oz./100 lb. of cement) as well as the typical dosage of the Type A water reducer Glenium 7500 (5.0 fl. oz./100 lb. of cement).

In addition to the control concrete listed above, two FR-SCC mixes were produced based on SCC mix designs developed at the Missouri University of Science and Technology and thorough trial and error at the University of Oklahoma. These mix designs specified a cement content of 750 lb., a Class C Fly Ash replacement of 30% by mass, a BASF MasterFiber MAC Matrix addition of 0.5% by volume, a water-to-cement ratio of 0.393, a target slump flow of 28 in., and a design air content of 6%. Citric Acid was also added every 10 minutes to help slow down the slump loss due to the Komponent. The only variation between the two FR-SCC mixes was the value of Komponent replacement. The two replacement levels considered were: 10% and 15% volumetric replacement of cement.

In order to help achieve the target slump flow and design air content, the mix design called for the typical SCC dosage range of ODOT-approved air entertainer MB-AE 90 (1.0-2.0 fl. oz./100 lb. of cement) as well as the typical dosage of the Type A water reducer Glenium 7500 (5.0-12.0 fl. oz./100 lb. of cement). The BASF MasterFiber MAC Matrix fibers used are macrosynthetic fibers that meet the requirments of ASTM C 1116 *Standard Specification for Fiber-Reinforced Concrete."* They are macro polypropylene fibers with an average length of 2.1 inches. The complete data sheet is listed in Appendix A.

3.3.1 Control Mix Design and Concrete Properties

A mix meeting the requirements of ODOT Class AA was used for the control mix in this study. The target strength was 4000 psi. The control mix

specifications are summarized in Table 3.1, and the oven-dry design batch weights are shown in Table 3.2. The fresh properties of the concrete were determined after the addition of the chemical admixtures on the day of casting the control beam specimens. The slump was 2.5 in., the air content was 4%, and the unit weight was 150.4 lb./ft^3.

Table 3.1 Control Mix Design Specifications

Cementitious Amount, lb./yd^3	588.0
Class F Fly Ash Replacement (by mass), %	20.0
w/c Ratio	0.34
Amount of Fine Aggregate (by volume), %	40.0
Design Air Content, %	6.0
Target Slump, in.	3.0

Table 3.2 Control Mix Design Proportions, Oven-Dry Basis

Cement	470.0 lb./yd^3
Class F Fly Ash	118.0 lb./yd^3
Water	200.0 lb./yd^3
Fine Aggregate	1323.0 lb./yd^3
Coarse Aggregate	1857.0 lb./yd^3
Air Entertainer MB-AE 90	0.75 fl. oz./cwt
Water Reducer Glenium 7500	4.54 fl. oz./cwt

The compressive strength, splitting tensile strength, and modulus of elasticity of the mix were determined from companion cylinders that were cast from the same concrete batch as the beam specimens. Figure 3.7 shows the compressive strength gain over time. At 28 days, the day of testing, the compressive strength was 6740 psi, well over the target strength. The modulus of elasticity of the concrete was determined to be 4540 ksi. The splitting tensile strength at 28 days was 459 psi.

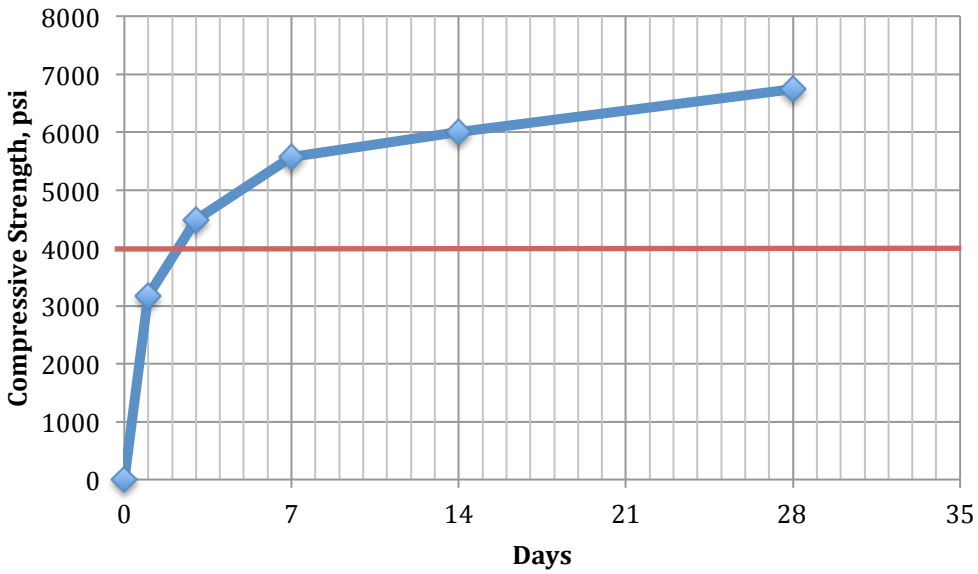

Figure 3.7 Control Mix Strength Gain with Time

3.3.2 10% Komponent FR-SCC Mix Design and Concrete Properties

The first FR-SCC mix incorporated 10% Komponent replacement. The target strength of the mix was 4000 psi. The mix specifications developed are summarized in Table 3.3, and the oven-dry design batch weights are shown in Table 3.4. The fresh properties of the concrete were determined after the addition of the chemical admixtures on the day of casting. The slump flow was 32 in. with no segregation, the air content was 9%, and the unit weight was 122.7 lb/ft^3.

Table 3.3 10% Komponent Mix Design Specification

Cementitious Amount, lb./yd^3	750.0
Class C Fly Ash Replacement (by mass), %	30.0
Komponent Replacement (by mass), %	10.0
w/c Ratio	0.39
Amount of Fine Aggregate (by volume), %	50.0
MasterFiber MAC Matrix (by volume), %	0.5
Design Air Content, %	6.0
Target Slump Flow, in.	28.0
Citric Acid (by mass), % of Komponent	0.35

Table 3.4 10% Komponent Mix Design Proportions, Oven-Dry Basis

Cement	450.9 lb./yd^3
Class C Fly Ash	224.1 lb./yd^3
Komponent	75.6 lb./yd^3
Water	177.2 lb./yd^3
Fine Aggregate	1401.3 lb./yd^3
Coarse Aggregate	1223.1 lb./yd^3
MasterFiber MAC Matrix	7.7 lb./yd^3
Air Entertainer MB-AE 90	1.1 fl. oz./cwt
Water Reducer Glenium 7500	9.0 fl. oz./cwt

The compressive strength, splitting tensile strength, and modulus of elasticity of the mix were determined from companion cylinders that were cast from the same concrete batch as the repair specimens. Figure 3.8 shows the compressive strength gain over time. At 28 days, the day of testing, the compressive strength was 4740 psi, just over the target strength. The modulus of elasticity of the concrete was determined to be 3952 ksi. The splitting tensile strength at 28 days was 406 psi.

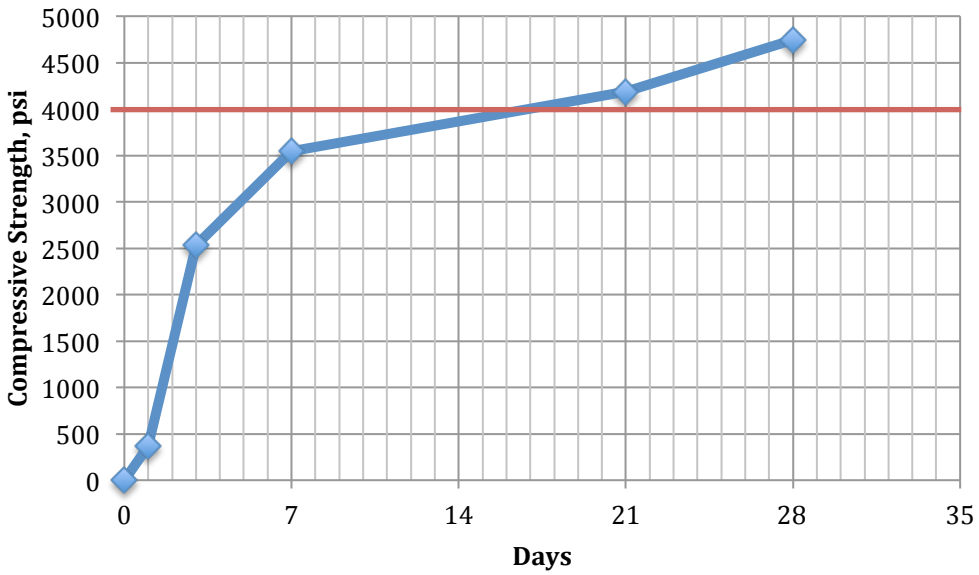

Figure 3.8 10% Komponent Mix Strength Gain with Time

3.3.3 15% Komponent FR-SCC Mix Design and Concrete Properties

The second FR-SCC mix incorporated 15% Komponent replacement. The target strength was once again 4000 psi. The mix specifications are summarized in Table 3.5, and the oven-dry design batch weights are shown in Table 3.6. The fresh properties of the concrete were determined after the addition of the chemical admixtures on the day of casting. The slump flow was 30 in. with no segregation, the air content was 10.5%, and the unit weight was 138.71 lb/ft^3.

Table 3.5 15% Komponent Mix Design Specifications

Cementitious Amount, lb./yd^3	750.0
Class C Fly Ash Replacement (by mass), %	30.0
Komponent Replacement (by mass), %	15.0
w/c Ratio	0.39
Amount of Fine Aggregate (by volume), %	50.0
MasterFiber MAC Matrix (by volume), %	0.5
Design Air Content, %	6.0
Target Slump Flow, in.	28.0
Citric Acid (by mass), % of Komponent	0.35

Table 3.6 15% Komponent Mix Design Proportions, Oven-Dry Basis

Cement	413.1 lb./yd^3
Class C Fly Ash	224.1 lb./yd^3
Komponent	113.4 lb./yd^3
Water	177.2 lb./yd^3
Fine Aggregate	1401.3 lb./yd^3
Coarse Aggregate	1223.1 lb./yd^3
MasterFiber MAC Matrix	7.7 lb./yd^3
Air Entertainer MB-AE 90	1.1 fl. oz./cwt
Water Reducer Glenium 7500	9.0 fl. oz./cwt

The compressive strength, splitting tensile strength, and modulus of elasticity of the mix were determined from companion cylinders that were cast from the same concrete batch as the repair specimens. Figure 3.9 shows the compressive strength gain over time. At test day, the compressive strength was 6010 psi, well over the target strength. The modulus of elasticity of the concrete was determined to be 4081 ksi. The splitting tensile strength at 28 days was 511 psi.

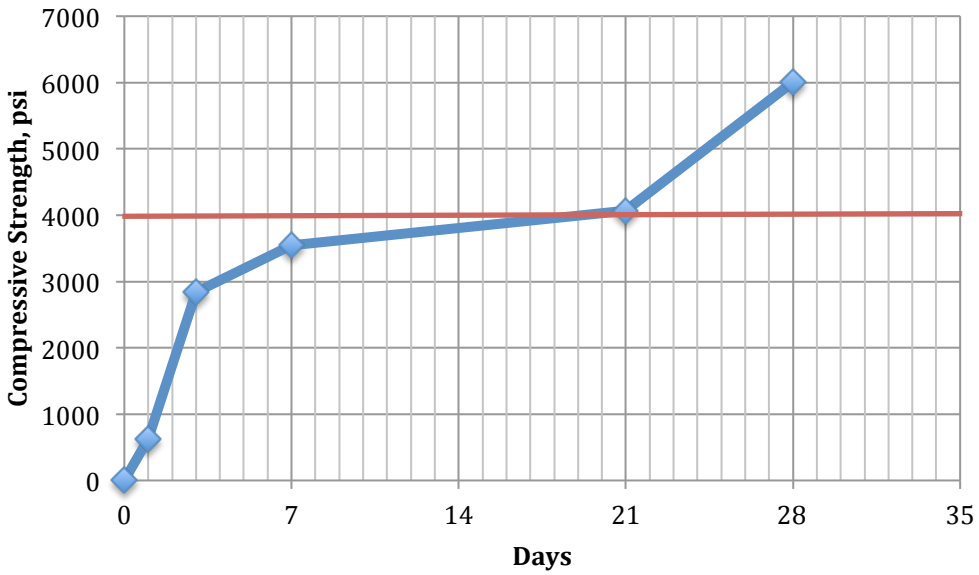

Figure 3.9 15% Komponent Mix Strength Gain with Time

3.4 CONCRETE MECHANICAL PROPERTIES

3.4.1 Modulus of Rupture Results

The modulus of rupture, f_r, of the control, 10% Komponent replacement, and 15% Komponent replacement concretes are shown in Table 3.7 along with the corresponding compressive strengths on the day of testing. The modulus of rupture for each mix was determined from the same mix as the repair specimens. In order to compare the test results across mix designs, the moduli of rupture were normalized by dividing the test value by the square root of the concrete compressive strength. This method of normalization is based on the accepted relationship between modulus of rupture and compressive strength as presented in ACI 318R (2014):

$$f_r = 7.5\lambda\sqrt{f'_c} \quad \text{(Eq. 3.3)}$$

where λ is a correction factor for lightweight concrete.

Table 3.7 Modulus of Rupture Results

Mix	f'$_c$ (psi)	f$_r$ (psi)	Normalized f$_r$	Average Normalized f$_r$
Control	6740	698.1	8.4	8.8
		777.4	9.5	
		693.6	8.5	
10% Komponent	4740	479.8	7.0	8.1
		590.9	8.6	
		607.1	8.8	
15% Komponent	6010	491.8	6.3	7.1
		590.3	7.6	
		563.2	7.3	

3.4.2 Modulus of Elasticity Results

The modulus of elasticity, E_c, of the control, 10% Komponent replacement, and 15% Komponent replacement concretes are shown in Table 3.8 along with the corresponding compressive strengths on the day of testing. The modulus of elasticity for each mix was determined from companion cylinders of the same mix as the repair specimens. In order to compare the test results across mix designs, the moduli of elasticity were normalized by dividing the test value by the square root of the concrete compressive strength. This method of normalization is based on the known relationship between modulus of elasticity and compressive strength as presented in ACI 318R (2014):

$$E_c = w_c^{1.5} 33\sqrt{f'_c} \quad \text{(Eq. 3.4)}$$

where w_c is the unit weight of the concrete.

Table 3.8 Modulus of Elasticity Results

Mix	f'c (psi)	Average MOE (ksi)	Average Normalized MOE
Control	6740	4540	55.3
10% Komponent	4740	3952	57.4
15% Komponent	6010	4081	52.7

3.4.3 Splitting Tensile Results

The splitting tensile strength, f_{tsp}, of the control, 10% Komponent replacement, and 15% Komponent replacement concretes are shown in Table 3.9 along with the corresponding compressive strengths on the day of testing. The splitting tensile strength of each mix was determined with companion cylinders of the same mix as the repair sections. To compare the results across mix designs, the splitting tensile strengths were normalized by dividing the test value by $f_c^{2/3}$. This method of normalization is based on the relationship between splitting tensile strength and compressive strength as presented in CEB-FIP (1999):

$$f_{tsp} = 1.57 f_c^{2/3} \quad \text{(Eq. 3.5)}$$

Table 3.9 Splitting Tensile Strength Results

Mix	f'c (psi)	Average f_{tsp} (ksi)	Average Normalized f_{tsp}
Control	6740	459.1	1.3
10% Komponent	4740	406.3	1.4
15% Komponent	6010	511.4	1.5

3.4.4 Comparison of Mechanical Properties

Figure 3.10 shows a graphical comparison of the mechanical properties of the three mixes. Each property was impacted differently with increasing Komponent replacement and the addition of fibers. The most drastic changes among mix designs were seen in the splitting tensile strength and the modulus of rupture. For splitting tensile strength, the introduction of fibers helped lead to an increase in tensile strength of 8% and 15% for the 10% Komponent replacement and the 15% Komponent replacement, respectively. The fibers, which only contribute to the tensile strength of the concrete, help hold any tension cracks together increasing the cracking strength and in turn the tensile strength of the concrete. The increased levels of Komponent help suspend the fibers within the concrete. The faster the concrete begins to set up (higher Komponent levels lead to a quicker slump loss and therefore lower ability for fibers to settle out), the more random the orientation and distribution of fibers becomes. This leads to a higher possibility of fibers crossing any single tension crack. Interestingly, the introduction of Komponenet seemed to have the opposite effect for modulus of rupture however. The modulus of rupture was decreased by 8% and 19% for 10% Komponent replacement and 15% Komponent replacement respectively. However these results still met the minimum standards in order to proceed with the study.

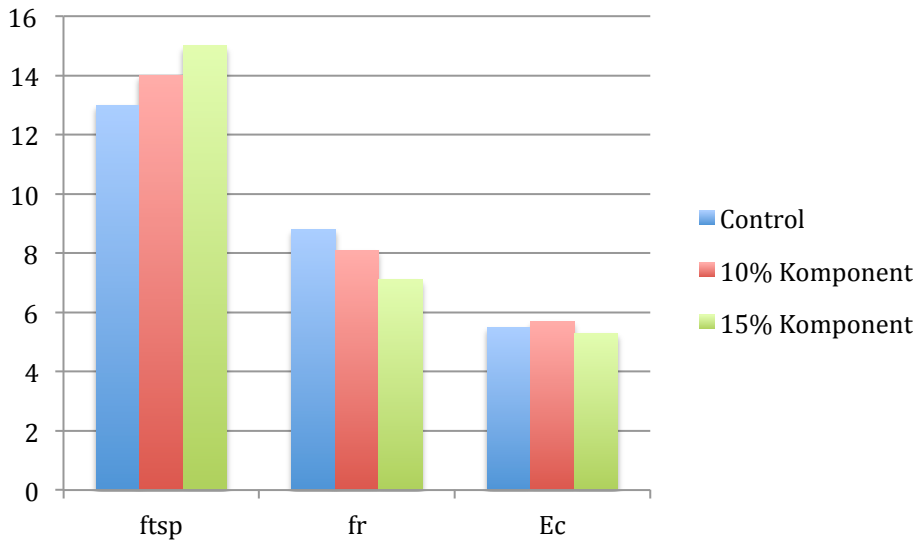

Figure 3.10 Comparison of Normalized Mechanical Properties

Note: Normalized values of $f_{tsp}*10$ and E_c*10^{-1}

4. FULL-SCALE EXPERIMENTAL PROGRAM

4.1 INTRODUCTION

In order to evaluate the cracking resistance and structural performance of FR-SCC in the use of bridge substructure repair, three sets of large-scale structural performance tests were performed: one set of monolithic control beams used as a standard to compare all FR-SCC results to, and two sets of FR-SCC repair beams based on the mix designs developed earlier.

4.2 CONTROL BEAM SPECIMENS

4.2.1 Control Beam Specimen Design

The design and fabrication of the control beam specimens was based on previous research of SCC flexural repairs (Kassimi, 2014). The beams used in this study were 14 ft. long with a cross section of 12 in. x 18 in. The longitudinal reinforcement consisted of four ASTM A615-09, Grade 60, #6 steel reinforcing bars. Transverse reinforcement against shear failure consisted of #3, ASTM A615-09, Grade 60, U-shaped stirrups. To ensure that a shear failure would not occur before flexural failure, a stirrup spacing slightly less than the ACI 318-11 maximum stirrup spacing was used. Figures 4.1 and 4.2 detail the cross-sectional and elevation views of the control beam specimens, respectively. As illustrated below, hooks were used at the free ends of the U-stirrups and #4 bars were used as top bars to help stabilize and align the cages.

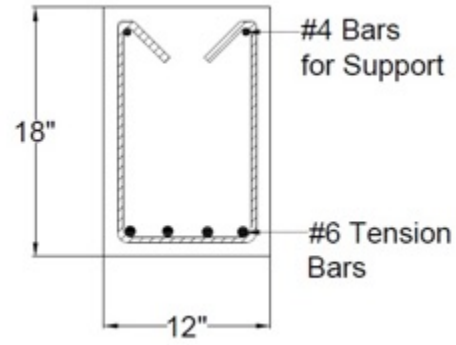

Figure 4.1 Control Beam Specimen Cross-Section

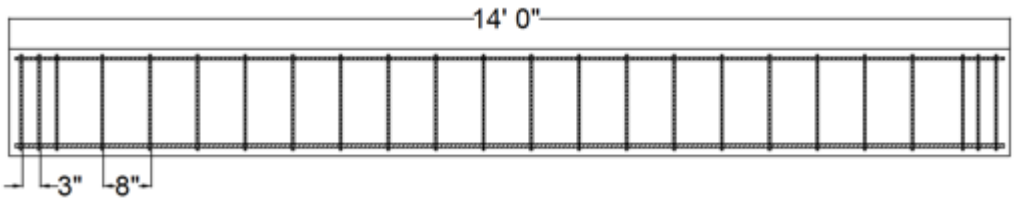

Figure 4.2 Control Beam Elevation

4.2.2 Control Beam Specimen Fabrication

Fabrication of the control beams began by building the steel cages needed to meet the design outlined earlier. Sawhorses were used to lay out the bottom reinforcement and were marked with a silver marker to denote the location of the stirrups. The stirrups were then placed along the longitudinal bars at these marked locations and the top bars were placed in the stirrup hooks. Once all bars and stirrups were in the correct place, wire ties were used to connect every joint of the cages (Figure 4.3). To ensure the appropriate cover was achieved during

casting, 1-in.-tall steel reinforcing chairs were tied to the bottom and sides of the cages.

Figure 4.3 Tying Steel Cage Joints

Once the steel cages were completed, strain gauges were attached to the outer tension bars at the mid-span location. Prior to attaching the strain gauges, the location of the gauges was prepared by grinding a smooth surface, cleaning the area with rubbing alcohol, and then wiping the area dry with a clean paper towel. The gauges were then attached to the steel using a cyanoacrylate adhesive (Figure 4.4) and then coated with a two-part epoxy adhesive. After the outer adhesive cured, the gages were wrapped in a buthyl rubber tape and then wrapped again in aluminum foil tape as shown in Figure 4.5.

Figure 4.4 Strain Gauge on Tension Bars

Figure 4.5 Wrapped Strain Gauge

Steel-framed forms with wood sides were used to construct the control beam specimens. The forms were held together by steel wedge bolts and ties, as well as steel straps across the top to prevent them from pulling apart during casting. The forms were then coated in form release oil to help facilitate de-molding. The cages were then lifted into the forms and the strain gauge wires were attached to the side of the form to prevent any damage. Figure 4.6 shows the completed cages inside the forms.

Figure 4.6 Completed Cages Inside Forms

Because a standard ODOT Class AA mix design was being used, the concrete was delivered to the lab by Dolese Brothers, a local ready mix plant. Upon the arrival of the concrete, the slump was measured in order to verify that the mix was correct. Once the mix was verified, the concrete was placed into a concrete bucket, which was used to fill the concrete forms as shown in Figure 4.7. While the forms were being filled, a wheelbarrow was filled with fresh concrete to be used for the air content test and to cast cylinders and prisms for the compression, splitting tensile, and MOR tests.

Figure 4.7 Concrete Bucket Filling Forms

The concrete was vibrated in layers to help consolidate it in the forms. Once filled, wood blocks were used to screed the surface of the beams and

finishing floats were used to smooth and level the top surface of each beam. As with the rest of the casting process, care was taken to avoid damage to the strain gauge wires. The forms were then covered with wet burlap and a tarp and were allowed to moist cure overnight.

The following day, the beams were removed from the forms and were once again covered with wet burlap and wrapped in a tarp for the remainder of the 7-day wet curing process. After 7 days, the beams were then allowed to cure in the laboratory, open to the air, for another 21 days prior to testing.

On the day before testing, the beams were prepared by applying a white latex coat of paint to facilitate viewing of the cracks as they appeared. Lines were also drawn to denote the locations of the supports and load points. Finally, two aluminum angles were attached to the concrete on the side of the beams at midspan so that the deflection could be monitored during testing.

4.2.3 Control Beam Specimen Test Set-Up

In accordance with the most common flexural tests, third-point loading was used in order to create a maximum constant moment in the middle third of the beam. Figure 4.8 shows the schematic of the third-point loading set-up used for the control beam specimens. The beam was loaded into the test frame using the overhead 5-ton crane as well as the roller supports that it would be resting on during the test. It was carefully placed under the load frame along the centerline of the steel support beam and centered under the overhead hydraulic jack. A 4-ft.-long spreader beam was used to transfer the applied load from the hydraulic

ram to the control beam specimen. Rollers were placed on top of the beam at the location of the third points and extra fine natural sand was placed beneath them to account for any roughness along the top of the concrete beam and allow for a level loading surface. Placed on top of the spreader beam was a greased pivot point, allowing for positive contact between the load and the spreader beam at any slight angle, as well as a 100 kip load cell as shown in Figure 4.9.

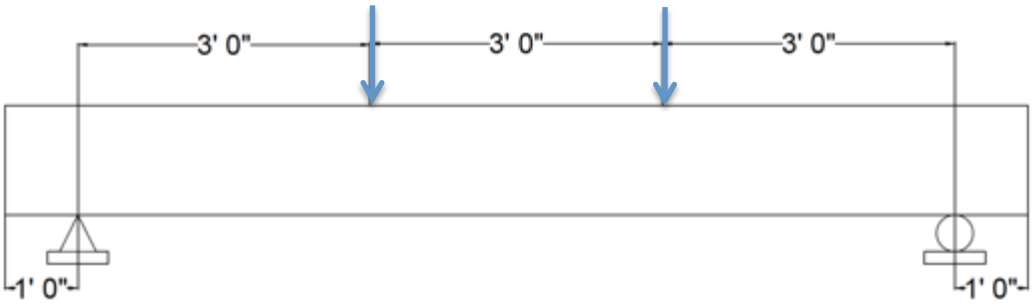

Figure 4.8 Control Beam Test Schematic

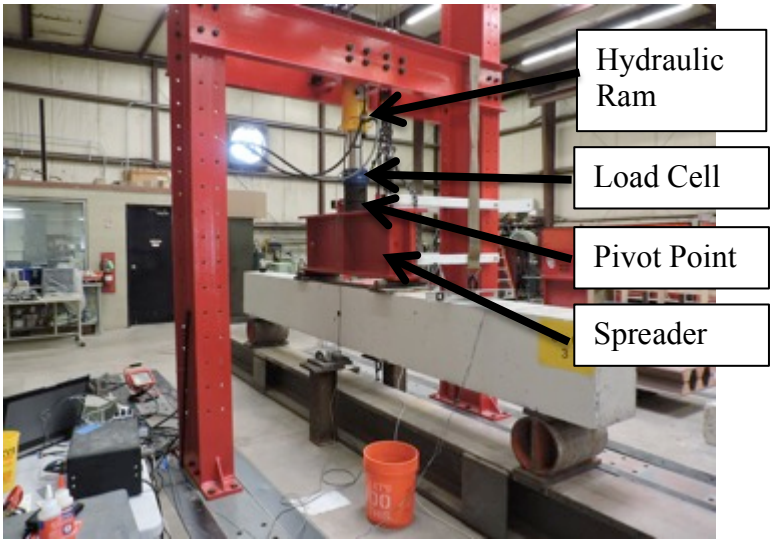

Figure 4.9 Control Beam Load Set-Up

String pots were attached to two steel stands on each side of the beam and the pin was attached to the aluminum angle that had been previously attached at the midspan location. This complete set up is shown in Figure 4.10. The string pots, as well as the two strain gauges, were then connected to the data acquisition channels and prepared for testing.

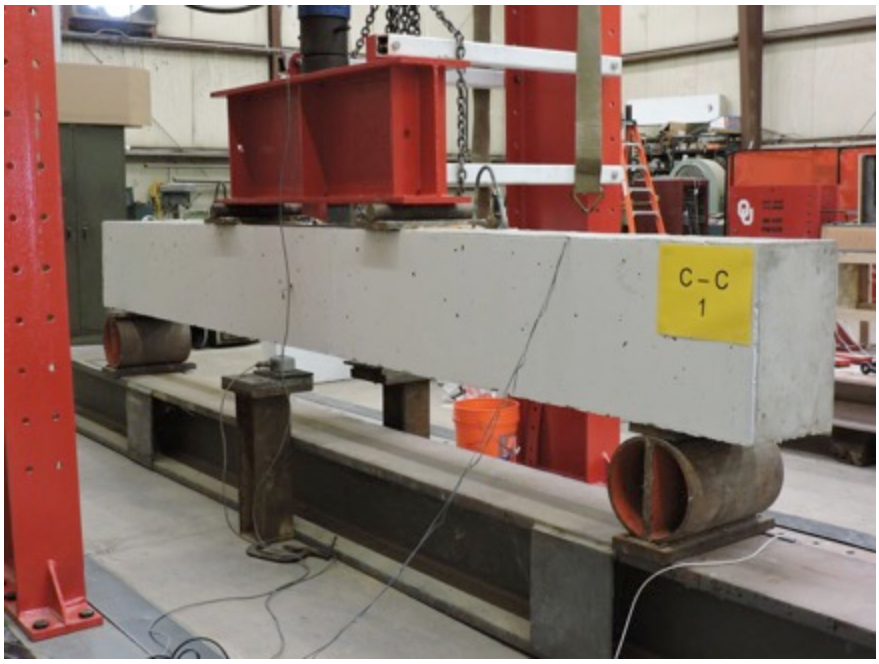

Figure 4.10 Control Beam Test Set-Up

4.2.4 Control Beam Test Procedure

To start the test, the data acquisition system was initiated to record all data from the strain gauges and string pots as well as the applied load through the load cell. The test was performed on a load-controlled basis; the load was applied in a series of 10 kip increments up to a total load of 80 kips and then 5 kip

increments there after until failure. After each applied step, the crack patterns were traced and photographed in order to track crack propagation.

The beam was loaded until the flexural steel failed by excessive yielding. This failure was typically marked by an inability to sustain additional load on the specimen, or a crushing of the concrete within the center third of the beam along the top surface. In most cases the beam would continually deflect without taking additional load or failing completely, therefore arbitrary stopping points were established once the above failure conditions were met. Once this failure occurred, testing was completed and data collection was stopped.

4.3 FR-SCC REPAIR BEAM SPECIMENS

4.3.1 FR-SCC Repair Beam Specimen Design

The design and fabrication of the FR-SCC repair beam specimens was based on previous research of SCC flexural repairs (Kassimi, 2014). The beams used in this study were 14 ft. long with a cross section of 12 in. x 18 in. Along the bottom of the beams was a repair zone with an average depth of 6 in. The depth was chosen to represent the effective tension zone, which can be repaired given advanced corrosion of the bottom steel reinforcement. The depth was slightly sloped from 7 in. at one end of the beam to 5 in. at the other end to help the flow of the FR-SCC as it was poured in the 7-in.-void end. The longitudinal reinforcement consisted of four ASTM A615-09, Grade 60, #6 steel reinforcing bars. Transverse reinforcement against shear failure consisted of #3, ASTM

A615-09, Grade 60, U-shaped stirrups. To ensure that a shear failure would not occur before flexural failure, a stirrup spacing slightly less than the ACI 318-11 maximum stirrup spacing was used. In order to simulate a true repair of the flexural zone, the control concrete was cast first and then flipped so that the repair concrete would be cast along the bottom. In order to accomplish this step, two vertical 4-in.-diameter holes were located near each end of the control concrete, along with two 1-in.-diameter vent holes near the third points to help allow air to escape during the placement. In addition, two horizontal 1.5-in.-diameter holes were created as pick points to help move the beam around the lab. Finally, eight threaded rods with nuts on the ends were used as legs to hold the control beam at the proper height above the formwork for the repair portion casting. Figures 4.11 and 4.12 detail the cross-sectional and elevation views of the control beam specimens, respectively. As illustrated below, hooks were used at the free ends of the U-stirrups and #4 bars were used as top bars to help stabilize and align the cages.

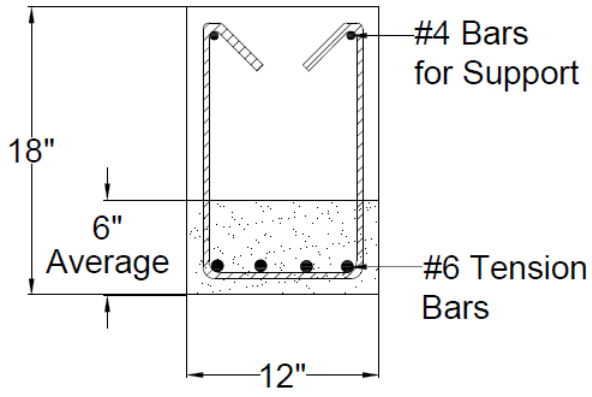

Figure 4.11 FR-SCC Repair Beam Cross-Section

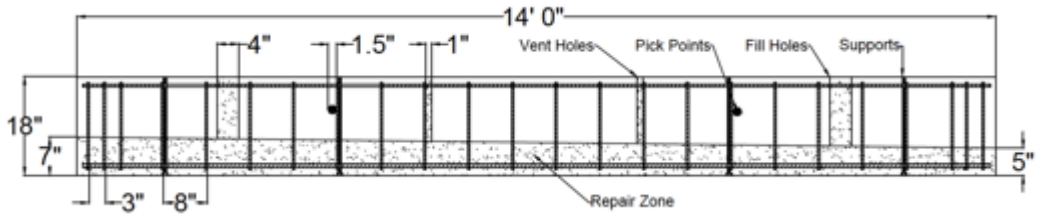

Figure 4.12 FR-SCC Repair Beam Elevation

4.3.2 FR-SCC Repair Beam Specimen Fabrication

The FR-SCC repair beams were cast in two separate layers: one representing the existing control concrete, and another representing the repair FR-SCC. Fabrication of the FR-SCC repair beams began by building the steel cages in a similar manner to the control beam specimens, however, prior to casting the control portion of the beam, the PVC pipes used for the vertical fill and vent holes and the horizontal pick points, as well as the threaded rod supports, were attached to the steel cage as shown in Figure 4.13. The cage was then placed inverted in the formwork with the tension reinforcement located near the top (Figure 4.14). Temporary tension bars were inserted for the control pour and the exposed portion of the stirrups was covered in electrical tape as shown in Figure 4.15. The tape prevented the reinforcement from coming in contact with any substrate concrete, assuring a good bond between the repair concrete and the reinforcement.

Figure 4.13 FR-SCC Repair Beam Cage

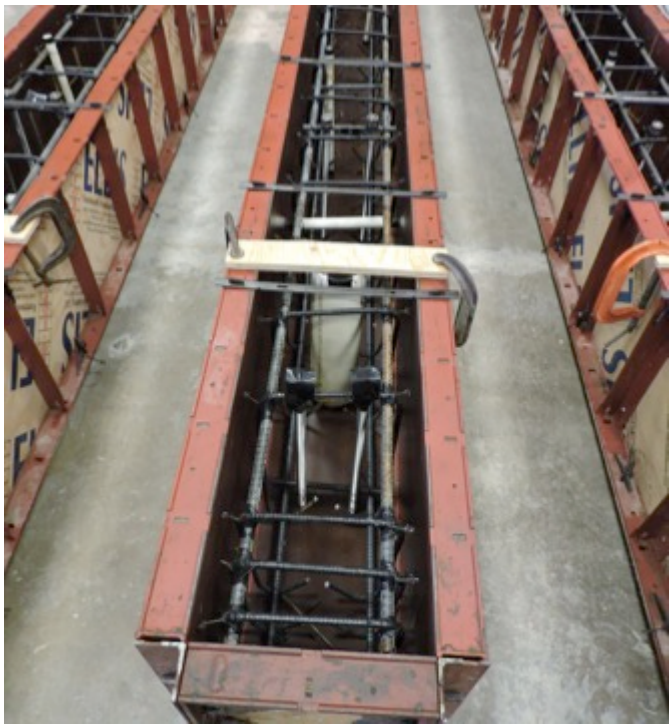

Figure 4.14 FR-SCC Cages in Forms

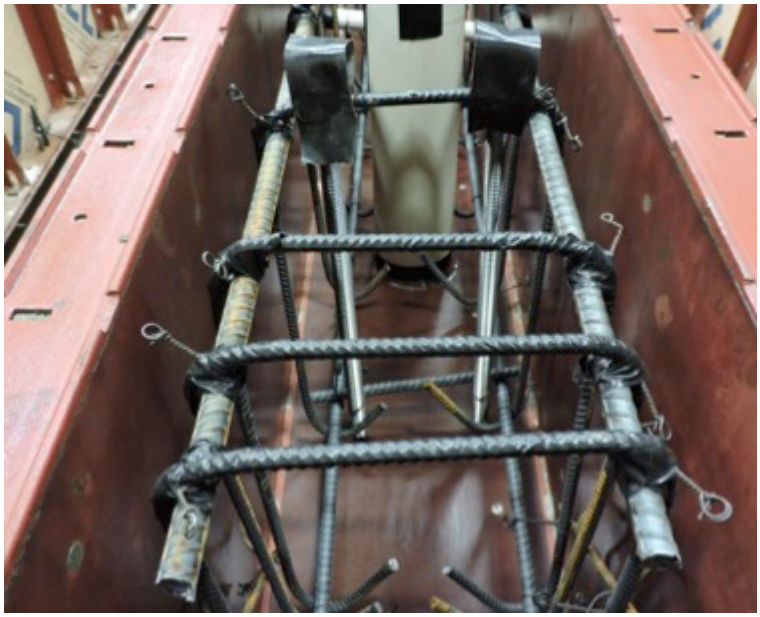

Figure 4.15 Stirrups Covered in Electrical Tape

The existing control portion of the beam was cast using the same ODOT Class AA sub-structure concrete mix as the control beam specimens and was delivered by Dolese Brothers. Upon the arrival of the concrete, the slump was measured in order to verify that the mix was correct. Once the mix was verified, the concrete was placed into a concrete bucket, which was used to fill the concrete forms. While the forms were being filled, a wheelbarrow was filled with fresh concrete to be used to perform the air content test and to cast cylinders and prisms for the compression, splitting tensile, and MOR tests.

The concrete was vibrated in layers to help consolidate it in the forms. The top surface was then sloped by measuring the distance from the top of the form to the top of the concrete as shown in Figure 4.16. Once the slope was

completed, a trowel edge was used to apply a roughened surface finish to the concrete to enhance mechanical bonding to the subsequent repair material (Figure 4.17). The concrete was then covered with wet burlap and a tarp and were allowed to moist cure overnight.

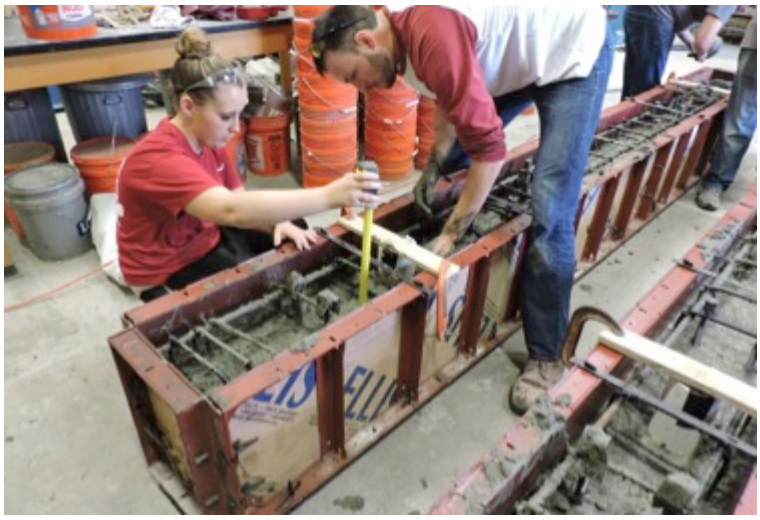

Figure 4.16 Measuring the Slope of the Control Concrete

Figure 4.17 Control Concrete Roughened Finish

The following day, the beams were removed from the forms and were once again covered with wet burlap and wrapped in a tarp for the remainder of the 7-day wet curing process. After 7 days, the beams were then allowed to cure in the laboratory, open to the air, for a minimum of another 21 days.

After curing was complete, the electrical tape and temporary tension bars were removed as well as the vertical PVC pipes being used for fill and vent holes. The exposed concrete was then cleaned using a power washer to expose coarse aggregate and enhance the bond to the repair material (Figure 4.18). Once cleaned, the beams were flipped right-side up so that the repair section was located near the bottom. The final tension reinforcement was then instrumented with strain gauges in a similar manner to the control beams and secured in place as shown in Figure 4.19. The partial beams were then placed on the base of the form (Figure 4.20) and the four sides were built up around each beam (Figure 4.21).

Figure 4.18 Power Washing the Concrete Surface

Figure 4.19 Beam Flipped and Tension Bars In Place

Figure 4.20 FR-SCC Repair Beam Placed on Form Bottom

Figure 4.21 FR-SCC Repair Beams Ready for Casting

On the day prior to casting, all the dry materials needed for the pour were batched, sealed, and brought inside to help maintain uniform moisture content and facilitate casting the following day. Samples were then taken from each of the aggregates and placed in the oven to obtain the exact moisture content on the day of casting.

On the day of mixing, all the materials needed to batch the FR-SCC were measured out based on the obtained moisture contents and final mix design developed previously. The mixer was watered down prior to mixing and was turned on so that the blades were spinning before any aggregate was added. The aggregate was then loaded in large buckets that could be either picked up by the

crane (Figure 4.22) or by the fork lift (Figure 4.23) and loaded into the mixer along with half of the required water. This material was then allowed to mix ensuring the aggregate was properly coated with water. The cement, fly ash, and Komponent were then added with the remainder of the water, with portions of the water added in between buckets of dry material. The concrete was then allowed to mix for 4 minutes prior to the addition of the Glenium 7500. The mixing cycle continued while the Glenium 7500 was added, followed by another minute of mixing prior to adding the fibers. Once the fibers were thoroughly distributed throughout the concrete, the citric acid was added and mixed for another minute. The citric was used to slow down the concrete slump loss.

Figure 4.22 Overhead Crane Bucket Transporting Fine Aggregate

Figure 4.23 Forklift Bucket Transporting Coarse Aggregate

Upon completion of the mixing process, the slump flow was performed in order to verify that the mix was performing as expected. Once the mix was verified, the concrete was placed into a concrete bucket, which was used to fill the repair area through a funnel inserted into the fill hole location, as shown in Figure 4.24. The large hole on the opposite side of the beam was used to monitor the flow of the FR-SCC. While the repair areas were being filled, a wheelbarrow was filled with fresh concrete to be used for the air content test and to cast cylinders and prisms for the compression, splitting tensile, and MOR tests.

Figure 4.24 Using the Funnel to fill FR-SCC Repair Sections

Once the repair area was filled, wood blocks were used to screed any excess concrete from the surface of the beams and finishing floats were used to smooth and level the fill and vent hole top surfaces. As with the rest of the casting process, care was taken to avoid damage to the strain gauge wires. The forms were then covered with wet burlap and a tarp and were allowed to cure overnight.

The following day, the beams were removed from the forms (Figure 4.25) and were once again covered with wet burlap and wrapped in a tarp for the remainder of the 7-day wet curing process. After 7 days, the beams were then allowed to cure in the laboratory, open to the air, for a minimum of another 21 days prior to testing.

Figure 4.25 FR-SCC Repair Beam Removed from Form

On the day prior to testing, the beams were prepared by applying a white latex coat of paint to facilitate viewing of the cracks as they appeared. Lines were also drawn to denote the locations of the supports and load points, as well as one red line to denote the plane between the existing concrete and the repair region. Finally, two aluminum angles were attached to the concrete on the side of the beams at midspan so that the deflection could be monitored during testing.

4.3.3 FR-SCC Repair Beam Specimen Test Set-Up

In accordance with the control beam specimens and the most common flexural tests, third-point loading was used in order to create a maximum constant moment in the middle third of the beam. Figure 4.26 shows the schematic of the third-point loading set-up used for the FR-SCC repair specimens. The beam was loaded into the test frame using the overhead 5-ton crane as well as the roller supports that it would be resting on during the test. It was carefully placed under the load frame along the centerline of the steel support beam and centered under the overhead hydraulic jack. A 4-ft.-long spreader beam was used to transfer the

applied load from the hydraulic ram to the control beam specimen. Rollers were placed on top of the beam at the location of the third points and extra fine natural sand was placed beneath them to account for any roughness along the top of the concrete beam and allow for a level loading surface. Placed on top of the spreader beam was a greased pivot point, allowing for positive contact between the load and the spreader beam at any slight angle, as well as a 100 kip load cell.

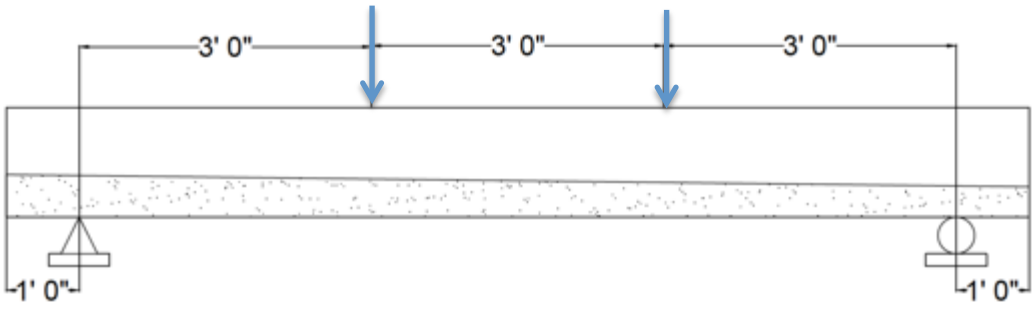

Figure 4.26 FR-SCC Repair Beam Test Schematic

String pots were attached to two steel stands on each side of the beam and the pin was attached to the aluminum angle that had been previously attached at the midspan location. This complete set up is shown in Figure 4.27. The string pots, as well as the two strain gauges, were then connected to the data acquisition channels and prepared for testing.

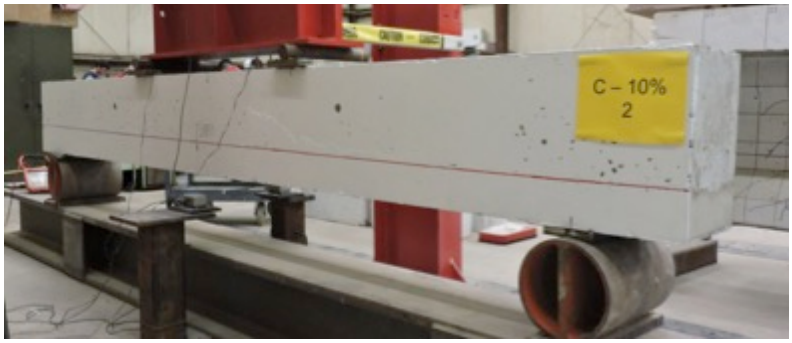

Figure 4.27 FR-SCC Repair Beam Test Set-Up

4.3.4 FR-SCC Repair Beam Test Procedure

The FR-SCC repair beam specimens were tested in a similar manner to the control beam specimens. To start the test, the data acquisition system was initiated to record all data from the strain gauges and string pots as well as the applied load through the load cell. The test was performed on a load-controlled basis; the load was applied in a series of 10 kip increments up to a total load of 80 kips and then 5 kip increments there after until failure. After each applied step, the crack patterns were traced and photographed in order to track the crack propagation.

The beam was loaded until the flexural steel failed by excessive yielding. This failure was typically marked by an inability to sustain additional load on the specimen, or a crushing of the concrete within the center third of the beam along the top surface. Similar to the control beams, in most cases the beam would continually deflect without taking additional load or failing completely, therefore arbitrary stopping points were established once the above failure conditions were met. Once this failure occurred, testing was completed and data collection was stopped.

5. TEST RESULTS AND EVALUATIONS

5.1 INTRODUCTION

In order to evaluate the cracking resistance and structural performance of FR-SCC in the use of bridge substructure repair, two repair based small-scale testes were performed in addition to the three sets of beams described and developed earlier in Chapter 4: one set of monolithic control beams used as a standard to compare all FR-SCC results to, and two sets of FR-SCC repair beams based on the mix designs developed in Chapter 3.

5.2 SMALL-SCALE REPAIR TEST RESULTS

In order to fully understand the structural compatibility of these repair sections to the control concrete, two sets of small-scale composite hardened property tests were also designed and completed: a third point loading composite prism test and a bond strength test.

5.2.1 Third Point Loading Composite Prism Test

Three concrete prisms, 20 in. in length with a cross section of 6 in. x 6 in., were cast in accordance with ASTM C 78 *Standard Test Method for Flexural Strength of Concrete.* The composite prisms were fabricated for the evaluation of the compatibility of the repair material with the substrate concrete and were fabricated in a similar manner to the same dimensional prism as the control specimen outlined in Chapter 3, with the exception of a 3 in. x 6 in. x 20 in. repair cast along the bottom of the prism as shown in Figure 5.1. During the

casting process, the control section was cast upside down and then a trowel edge was used to apply a roughened surface finish to the concrete similar to the full-scale beams. After curing for at least 28 days with the control portion of the repair beams, the repair FR-SCC was cast on top of the control concrete creating a composite prism and cured in a similar manner to the full-scale repair beams described in Chapter 4. Once the curing process was complete, the composite sections were flipped to their final orientation before being tested.

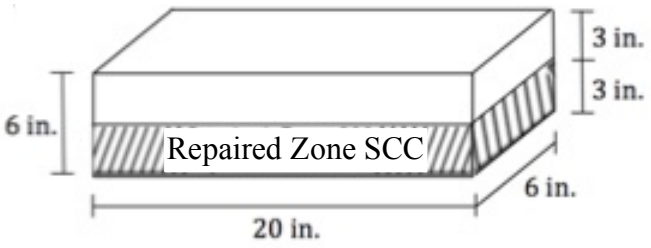

Figure 5.1 Third Point Loading Composite Prism

These composite prisms were then tested to determine a modulus of rupture, f_r, in accordance with ASTM C 78. To test these beams, simple third point loading was used with a span length of 18 in. as shown in Figure 5.2. Upon reaching the peak load of the test, the modulus of rupture was calculated by Equation 5.1:

$$f_r = \frac{P*L}{b*d^2} \qquad \text{(Eq. 5.1)}$$

where P is the peak load, L is the beam span, and b and d are the beam width and depth, respectively, measured at the fractured surface of the beam. Three composite specimens were tested for each repair FR-SCC with the average representing one strength data point.

Figure 5.2 Composite Modulus of Rupture Test Set-Up

The modulus of rupture, f_r, of the composite prims are shown in Table 5.1 along with the corresponding compressive strengths of the repair section on the day of testing. The repair compressive strengths were chosen because of its location in the tension zone of the prism, the critical area when developing modulus of rupture strengths.

Table 5.1 Composite Modulus of Rupture Results

Mix	f'_c (psi)	f_r (psi)	Normalized f_r	Average Normalized f_r
C-10%	4740	435.9	6.3	6.6
		467.4	6.8	
		463.5	6.7	
C-15%	6010	697.5	9.5	9.5
		624.7	8.5	
		756.9	10.3	

5.2.2 Bond Strength Test

The bond strength of the repair FR-SCC to the substrate control concrete was determined in accordance with ASTM C 882 *Standard Test Method for Bond Strength of Epoxy-Resin Systems Used With Concrete By Slant Shear.* The

repair FR-SCC was bonded to a substrate concrete specimen on a slanted elliptical plane at a 30-degree angle from the vertical to form a 6 in. x 12 in. composite cylinder as shown in Figure 5.3. The control portion of the cylinder was cast with the cylindrical mold placed on a carefully crafted incline table (Figure 5.4) and allowed to cure along with the control portion of their respective full-scale beams. Before casting the repair FR-SCC with the cylinder in the upright position, the slanted surface was cleaned and dried.

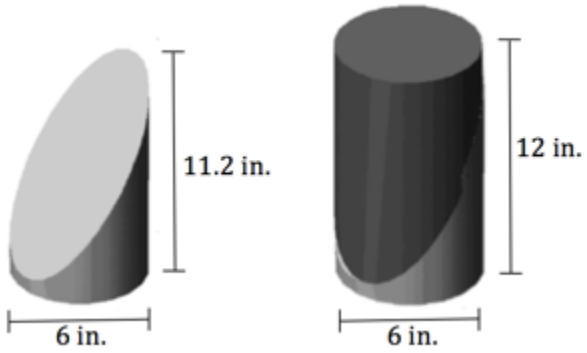

Figure 5.3 Bond Strength Test Specimen

Figure 5.4 Incline Table for Casting the Control Portion

These composite cylinders were then tested to determine a bond strength in accordance with ASTM C 882. First, the compressive strength of the concrete was determined as per ASTM C 39 Standard Test Method for Compressive Strength of Cylindrical Concrete Specimens. Prior to testing, the cylinders were ground down with the Marui Concrete Specimen End Grinder to give a uniform stress distribution during testing. The cylinders were then loaded between 28 psi/sec and 42 psi/sec as per the ASTM C 39 standard. Figure 5.5 shows a ground composite cylinder in the loading machine. Upon reaching the peak load of the test, as shown in Figure 5.6, the bond strength was calculated by Equation 5.2:

$$Bond\ Strength = \frac{P}{A_{surface}} \qquad \text{(Eq. 5.2)}$$

where P is the peak load and $A_{surface}$ is the area of the slanted failure plane accounting for any voids greater than 3 mm in diameter. Three specimens were tested with the average representing one strength data point.

Figure 5.5 Bond Strength Test Set-Up

Figure 5.6 Typical Bond Strength Failure

Table 5.2 Bond Strength Results

Mix	Peak Load (lbs)	Surface Area (in^2)	Bond Strength (psi)	Average Bond Strength (psi)
C-10%	111,945	242.4	461.9	475.9
	136,785	242.4	564.4	
	95,460	237.7	401.6	
C-15%	135,345	247.2	547.6	569.8
	143,410	240.3	596.7	
	137,905	244.0	565.1	

5.3 REBAR TESTING RESULTS

In order to determine the ultimate stress, yield stress, and modulus of elasticity of the reinforcing bars used in the full-scale beam specimens, tension tests were performed in accordance with ASTM E 8-09 *Standard Test Methods for Tension Testing of Metallic Materials.* This test was performed on three 36 in.

lengths of #6 reinforcing bars. Each specimen was clamped at each end in a 200 kip capacity load frame and loaded until rupture. Throughout testing, both strain and load were recorded. For each specimen, the yield stress of the bar was determined from the 0.2% strain offset of the stress versus strain plot. The modulus of elasticity was also determined for each bar using the slope of the linear portion of the stress strain curve. Table 5.3 shows the results of the #6 reinforcing bar tension test.

Table 5.3 #6 Reinforcing Bar Tension Test Results

Specimen	Yield Stress (ksi)	Average Yield Stress (ksi)	Ultimate Stress (ksi)	Average Ultimate Stress (ksi)	Modulus of Elasticity (ksi)	Average Modulus of Elasticity (ksi)
1	77.97	78.24	109.28	109.12	28,396	28,623
2	78.46		109.13		28,779	
3	78.28		108.96		28,694	

5.4 FULL-SCALE REPAIR TEST RESULTS

The full-scale beam specimens were constructed to provide a relative measure of flexural performance for the two sets of repair beams in comparison to a monolithic beam created from the ODOT Class AA control mix. For this experimental program, a total of 9 beam specimens were tested. One set of 3 control beams (C-C), and two sets of 3 repair beams representing FR-SCC with 10% Komponent replacement (C-10%) and 15% Komponent replacement (C-15%). The testing matrix is shown below in Table 5.4.

Table 5.4 Testing Matrix for Full-Scale Beams

Mix	Bottom Reinforcement	Top Reinforcement	Number of Beams
C-C	4 #6	2 #4	3
C-10%	4 #6	2 #4	3
C-15%	4 #6	2 #4	3

Throughout the flexural testing of the beam specimens, the midspan deflection, applied total load, and strain in the steel were recorded. Table 5.5 shows a summary of the structural performance results of the full-scale repair tests. Within each of the specimen names, C-C represents the Class AA control concrete, C-10% represents 10% Komponent replacement in the repair FR-SCC, and C-15% represents 15% Komponent replacement in the repair FR-SCC. The final number of the specimen name indicates which of the three tests that specimen was identified as.

Table 5.5 Full-Scale Beam Test Results

Mix	Specimen	Cracking Load (kips)	Avg. Cracking Load (kips)	Cracking Load COV	Peak Load (kips)	Avg. Peak Load (kips)	Peak Load COV
C-C	C-C-1	18.1	17.2	4.61%	94.2	94.2	0.33%
	C-C-2	16.6			93.9		
	C-C-3	16.9			94.6		
C-10%	C-10%-1	18.4	16.9	8.06%	91.1	91.2	1.13%
	C-10%-2	16.7			90.2		
	C-10%-3	15.7			92.3		
C-15%	C-15%-1	12.9	13.1	1.59%	90.2	90.1	0.02%
	C-15%-2	13.3			90.1		
	C-15%-3	13.2			90.1		

5.4.1 Load-Deflection Response

The load-deflection relationships of the monolithic control beams, as well as the 10% and 15% Komponent replacement repaired beams are shown in Figures 5.7, 5.8, and 5.9, respectively. The load-deflection relationship is tri-linear for each of the specimens. The first portion representing the behavior of the uncracked beam, which depends on the gross moment of inertia of the concrete cross-section, was similar for all beams. The second portion, representing the post-cracking section up to the steel yielding, corresponds to the cracked beam with a reduced moment of inertia. The final portion, representing the steel yielding up to failure, corresponds to degradation in the stiffness of the beams due in part to the yielding of the tension bars. In most cases the beam would continually deflect without taking additional load or failing completely, therefore arbitrary stopping points were established once the steel yielded or the concrete began to crush. It was determined that the load-deflection response was more integral to the evaluation of the flexural behavior of our specimens, and in turn the completion of the objectives stated earlier, therefore the steel strain diagrams monitored throughout the test were only used to help determine this steel yielding failure point. However, the steel strain responses are all listed for reference in Appendix B.

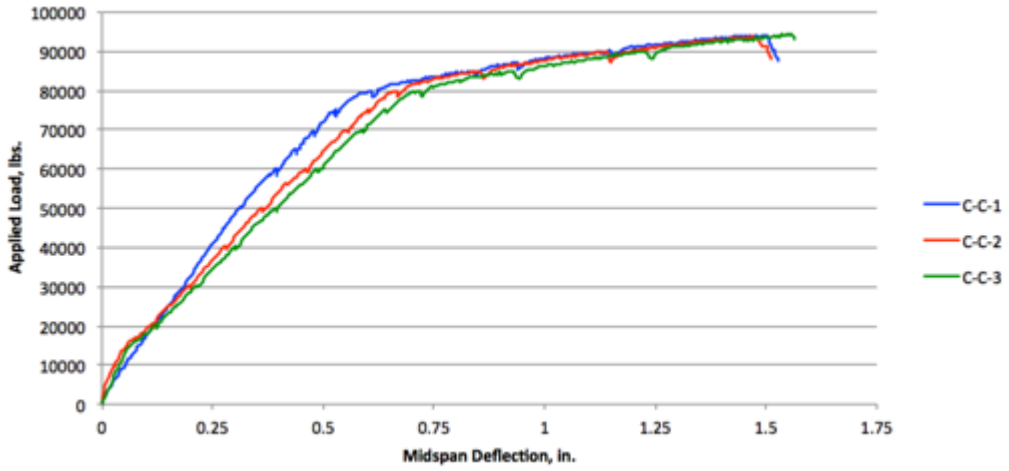

Figure 5.7 Control Monolithic Beam Load vs. Deflection Plots

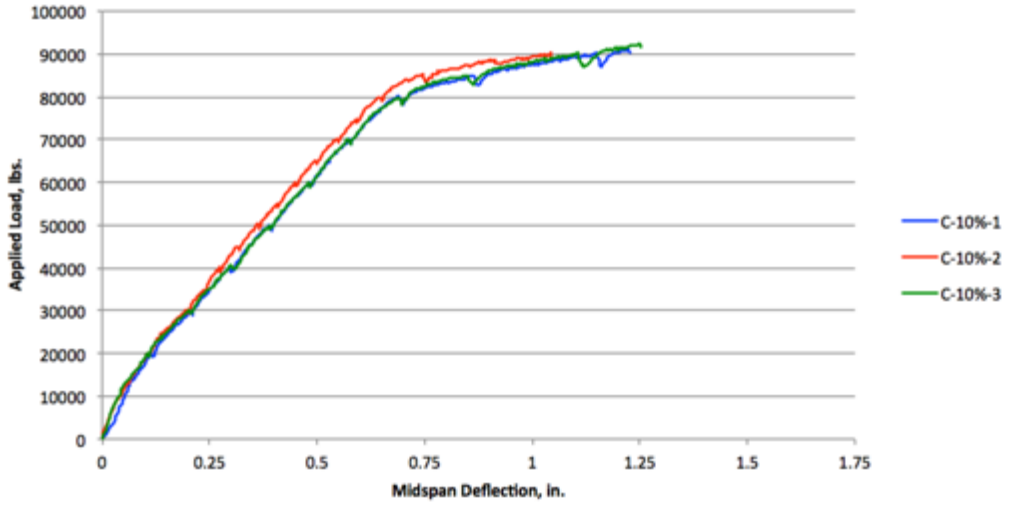

Figure 5.8 10% Komponent Replacement Load vs. Deflection Plots

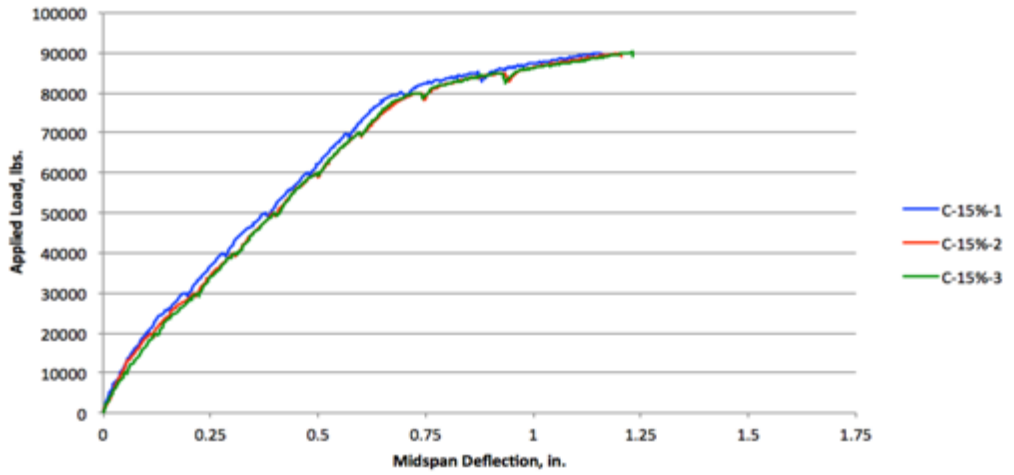

Figure 5.9 15% Komponent Replacement Load vs. Deflection Plots

5.4.2 Cracking Behavior and Strains

Similar cracking characteristics were observed for all 9 beams. Cracks were initiated within the flexural span between the two concentrated load points. This makes sense as this is where flexural stress is the highest and shear stress is at zero. The cracks were primarily vertical and perpendicular to the direction of the maximum tensile stress, induced by the pure bending of the beam. As the load was increase, additional flexural cracks started within the shear span; however, because of the presence of shear stresses, the cracks became progressively more inclined and moved towards the two concentrated load points. The beam typically failed by excessive yielding of the flexural steel. This failure was marked by an inability to sustain additional load on the specimen, or a crushing of the concrete within the center third of the beam along the top surface.

Figures 5.10 through 5.12 show the cracking patterns at failure of the tested beams. With some of the repaired beams, very thin horizontal cracks were observed in the interface between the substrate and repair concretes marked by the red line on the beam. The cracking load values were reported previously in Table 5.5.

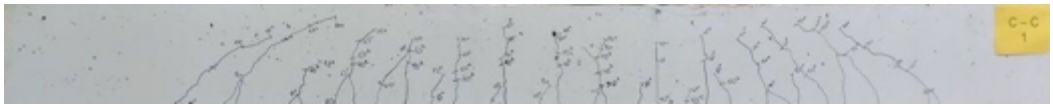

Figure 5.10a Cracking Pattern of C-C-1

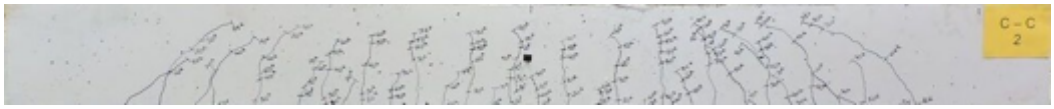

Figure 5.10b Cracking Pattern of C-C-2

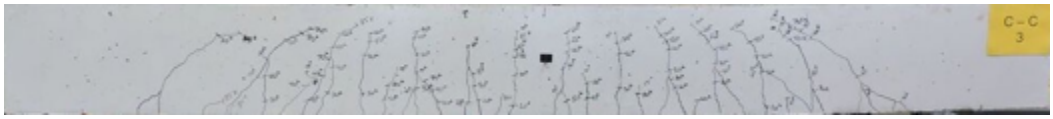

Figure 5.10c Cracking Pattern of C-C-3

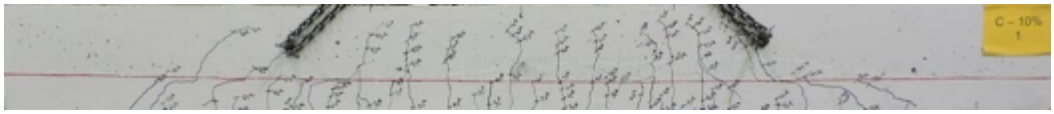

Figure 5.11a Cracking Pattern of C-10%-1

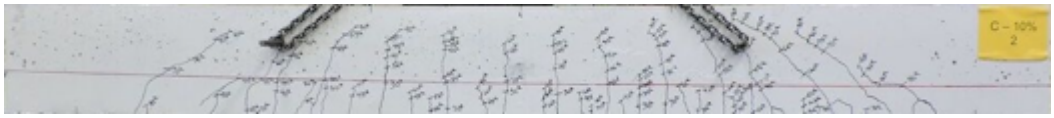

Figure 5.11b Cracking Pattern of C-10%-2

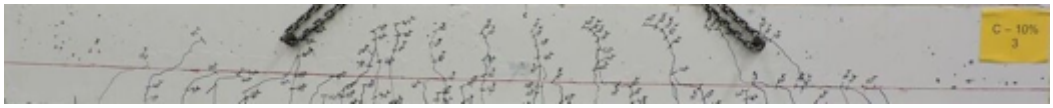

Figure 5.11c Cracking Pattern of C-10%-3

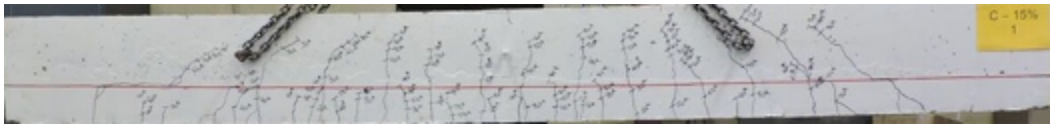

Figure 5.12a Cracking Pattern of C-15%-1

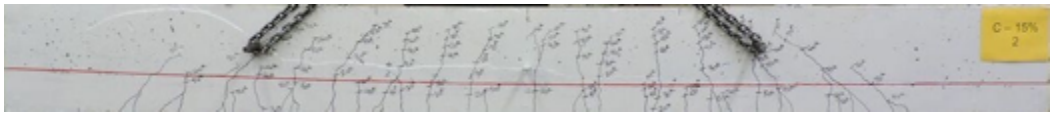

Figure 5.12b Cracking Pattern of C-15%-2

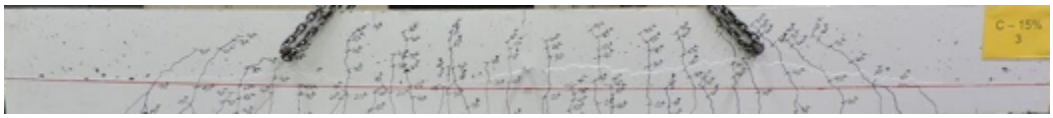

Figure 5.12c Cracking Pattern of C-15%-3

5.5 ANALYSIS OF RESULTS

5.5.1 Analysis and Interpretation of Small-Scale Results

The normalized results from the Third Point Loading Composite Prism Tests are shown in Table 5.6, which includes both the monolithic test results from Chapter 3 and the composite prism test results from this chapter. For the monolithic prisms, the repair mixes showed decreased modulus of rupture values compared to the control concrete. This result may have been due to the increased compressive strengths of the repair mixes due to the added Komponent that did not readily translate into a corresponding increase in modulus of rupture. Type K cements such as Komponent require substantially more water during curing, therefore a simple wet curing process as described in Chapter 4 might not have been adequate to properly hydrate the cement. Alternatively, the random

orientation of the fibers may have resulted in potential weak planes through the prisms, however this is the least likely explanation.

Table 5.6 Normalized Modulus of Rupture Results

Mix	Monolithic Prisms	Composite Prisms
C-C	8.8	-
C-10%	8.1	6.6
C-15%	7.1	9.5

However, as shown in Table 5.6, an increase in the Komponent replacement level led to a higher normalized modulus of rupture for the composite prism sections. Interestingly, this is the opposite from what happened during the monolithic modulus of rupture tests described in Chapter 3, but more in line with our expectations. Because Komponent is a shrinkage-compensating cement, the increased replacement could have led to fewer shrinkage cracks along the bond surface, therefore increasing the overall flexural strength of the prism. Because there was no bond surface to shrink away from in the monolithic prisms, this increase was not seen. The increased modulus of rupture strength could also be attributed to the suspension of fibers within the mix. As described in Chapter 3, the faster slump loss of higher Komponent replacement concretes could lead to a more random suspension of fibers within the concrete, therefore increasing the possibility that a fiber crosses any specific flexural crack.

The results from the Bond Strength Tests are shown in Table 5.7. Because there is a direct relationship between compressive strength and bond strength, there was no need to normalize these results. The bond strength

increased 20% for the C-15% mix compared to the C-10% mix while the corresponding compressive strength only increased 13%. Similar to the composite modulus of rupture tests, an increase in the Komponent replacement level led to a higher bond strength. As described earlier, this could be due to an improved bond between the control concrete and the FR-SCC repair concrete due to a reduction in shrinkage cracking. Because the specimen failed along the bond plane, it is unlikely that the distribution of fibers within the mix played a significant role in this increased strength.

Table 5.7 Bond Strength Test Results

Mix	Average Compressive Strength (psi)	Average Bond Strength (psi)
C-10%	4740	476
C-15%	6010	570

5.5.2 Analysis and Interpretation of Full-Scale Results

A summary of the structural performance results of the test beams is given in Table 5.8. The table includes the cracking and yielding moments obtained from the load versus deflection diagrams shown previously as well as the ultimate moment capacity obtained from the peak load data. A summary of the calculated cracking moment and ultimate moment capacity is then given in Table 5.9 along with a comparison to the experimental results.

As it can be seen in the following tables, the two sets of repair beams had lower experimental ultimate moments than the control beam, however they are

statistically equivalent with a Coefficient of Variation between the ultimate moments of only 2.6%. The experimental ultimate moments were also all within 5% of the calculated capacities as show in in Table 5.9. However, on the other hand the experimental cracking moments varied in comparison to the calculated moments for each set of specimens. The experimental cracking moment met or exceed the calculated moments for both the control specimens as well as the 10% Komponent replacement specimens. The experimental cracking moment of the 15% Komponent replacement was only 81% of the calculated moments. As described in the analysis and interpretation of the small-scale results, this could be due to the existence of a shrinkage plane along the bond surface. This shrinkage plane allows for shrinkage cracks to develop as the two separate concretes cure, shrink, and try to pull away from each other.

Table 5.8 Full-Scale Beam Test Results

Mix	Specimen	Experimental Results					
		M_{cr} (k-ft)	Avg. M_{cr} (k-ft)	M_y (k-ft)	Avg. M_y (k-ft)	M_u (k-ft)	Avg. M_u (k-ft)
C-C	C-C-1	36	33	162	164	188	189
	C-C-2	32		164		188	
	C-C-3	32		166		190	
C-10%	C-10%-1	36	33	162	164	182	182
	C-10%-2	32		166		180	
	C-10%-3	30		164		184	
C-15%	C-15%-1	24	25	162	165	180	180
	C-15%-2	26		166		180	
	C-15%-3	26		166		180	

Table 5.9 Full-Scale Beam Calculation Comparison Table

Mix	Calculated Results		M_{cr_exp}/M_{cr_calc}	M_{u_exp}/M_{u_calc}
	M_{cr} (k-ft)	M_u (k-ft)		
C-C	33	179	1.00	1.05
C-10%	28	174	1.18	1.04
C-15%	31	177	0.81	1.01

As shown in Figures 5.7 thru 5.9, the load-deflection response for the test specimens is very consistent for each concrete type. Figure 5.13 shows the load deflection response for one control specimen, one 10% Komponent specimen, and one 15% Komponent specimen. As shown in the figure, the load-deflection response is very similar between these concrete types. The control beams had a slightly lower deflection throughout the uncracked and post-cracking portions of the load-deflection response, however the deflections were relatively consistent once the steel-yielding region was reached.

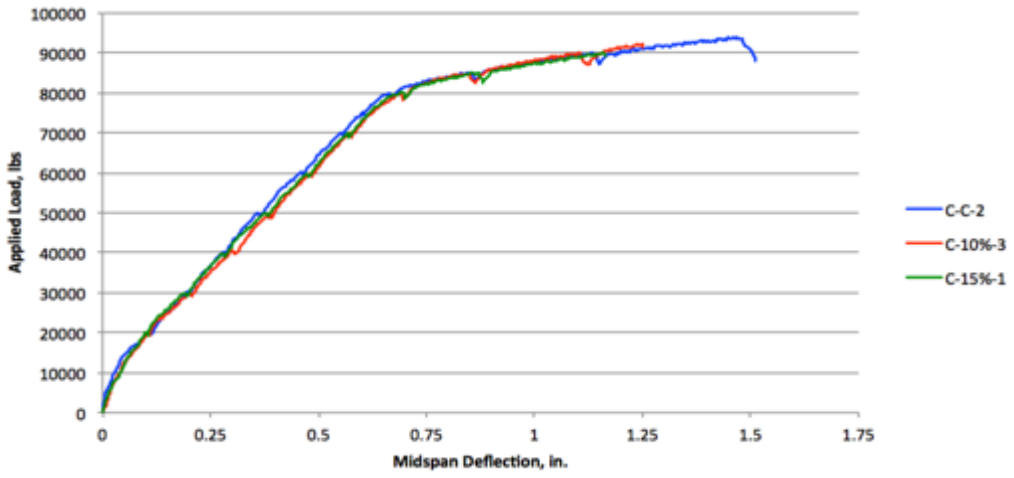

Figure 5.13 Load-Deflection Response Comparison

Comparing Figures 5.10a thru 5.12c, the extent and morphology of the cracking is very consistent between all the concrete types. In general, the flexure and flexure-shear cracks of the repair beams run directly through the interface between the two materials, indicating that the beams are acting monolithically. There are a few instances towards the shear region of the beam, however, where the cracks transverse horizontally a short distance before resuming their upward trend. This situation would indicate the possibility of a slight debonding or slippage between the repair material and the base concrete. It can also be attributed to the shear stresses in this area leading to an increase in tensile forces pulling the two concretes apart.

6. FINDINGS, CONCLUSIONS, AND RECOMMENDATIONS

6.1 INTRODUCTION

The objective of this study was to determine the structural behavior of bridge substructures retrofitted with FR-SCC tension zones. The following chapter presents the findings, conclusions, and recommendations of this study. The testing program compared FR-SCC repair mix designs at two different Komponent replacement levels: 10% replacement, denoted as C-10%, and 15% replacement, denoted as C-15%. A standard Oklahoma Department of Transportation (ODOT) Class AA mix design was used as a baseline control mix throughout the study.

In addition to material properties testing, both small-scale and full-scale repair tests were conducted. The small-scale repair tests included Third Point Loading Composite Prism Tests, modeled after the ASTM C 78 *Standard Test Method for Flexural Strength of Concrete,* as well as Bond Strength Tests modeled after ASTM C 882 *Standard Test Method for Bond Strength of Epoxy-Resin Systems Used With Concrete By Slant Shear.* The full-scale tests included a total of 9 beam specimens. One set of 3 control beams (C-C), and two sets of 3 repair beams representing FR-SCC with 10% Komponent replacement (C-10%) and 15% Komponent replacement (C-15%). While the small-scale tests provided a good indicator on how the two concretes were going to interact, the full-scale beams allowed for a more realistic stress state response in evaluating the flexural performance of these repairs.

6.2 FINDINGS

6.2.1 Material Properties Testing

Each of the hardened concrete properties of the various FR-SCC mixes that were described in Chapter 3 were impacted differently with increasing Komponent replacement, the addition of fibers, and the introduction of other admixtures to help create the flow properties of a self-consolidating mix. The most drastic changes among mix designs were seen in the splitting tensile strength and the modulus of rupture results. The splitting tensile strength increased by 8% and 15% for C-10% and C-15% respectively. The modulus of rupture, however, was decreased by 8% for C-10% and 19% for C-15%.

6.2.2 Small-Scale Repair Testing

For the Third Point Loading Composite Prism Tests in Chapter 5, comparisons to the monolithic modulus of rupture tests from Chapter 3 were made. For the monolithic prisms, the repair mixes showed decreased normalized modulus of rupture values compared to the control concrete. C-10% had an 8% reduction in modulus of rupture in comparison to the control concrete, while C-15% had a 20% reduction. However, the opposite occurred during the composite prism tests. An increase in the Komponent replacement level led to a normalized modulus of rupture increase of almost 44% from C-10% to C-15%.

For the Bond Strength Tests, the increased Komponent replacement levels led to higher bond strengths in relation to their respective compressive

strengths. The bond strength increased 20% for the C-15% mix compared to the C-10% mix while the corresponding compressive strength only increased 13%.

6.2.3 Full-Scale Repair Testing

The two sets of repair beams had lower experimental ultimate moments than the control beam, however they are statistically equivalent with a Coefficient of Variation between the ultimate moments of only 2.6%. The experimental ultimate moments were also all within 5% of the calculated expected capacities. However, on the other hand, the experimental cracking moments varied in comparison to the calculated moments for each set of specimens. The experimental cracking moment met or exceed the calculated moments for both the control specimens as well as the C-10% specimens. The experimental cracking moment of the C-15% was only 81% of the calculated moments.

The load-deflection response for the test specimens was very consistent for each concrete type. The control beams had a slightly lower deflection throughout the uncracked and post-cracking portions of the load-deflection response; however, the deflections were relatively consistent once the steel-yielding region was reached. The extent and morphology of the cracking was also very consistent between all the concrete types. In general, the flexure and flexure-shear cracks of the repair beams ran directly through the interface between the two materials, indicating that the beams were acting monolithically.

There were a few instances, however, where the cracks transversed horizontally a short distance along the interface before resuming their upward trend.

6.3 CONCLUSIONS

Overall, the two repair concretes, C-10% and C-15%, examined throughout this study showed comparable load-carrying capacities and cracking loads to monolithic control beams. The conclusions based on the findings of both the small-scale and full-scale tests described earlier are highlighted in the following sections.

6.3.1 Material Properties Testing

Analysis of the fresh and hardened concrete material properties indicates that highly workable FR-SCC can be made using synthetic fibers and local materials. The investigated mixtures fulfilled all the passing ability, filling capacity, and stability requirements needed to provide a successful repair.

The investigated fiber-reinforced self-consolidating concrete mixtures were found to be suitable for repair applications. They were able to flow horizontally under their own weight along the length of the 14 ft. beams and were able to achieve good compaction in the absence of vibration without exhibiting effects due to segregation and blockage.

6.3.2 Small-Scale Testing

Analysis of the small-scale test results indicates that both C-10% and C-15% repair concretes performed comparably to the control ODOT Class AA

concrete. For the monolithic prisms, the repair mixes showed a slight decrease in modulus of rupture value compared to the control concrete. This result may have been due to the increased compressive strengths of the repair mixes due to the added fibers that did not readily translate into a corresponding increase in modulus of rupture. In addition, self-desiccation due to our curing method could have also led to this reduction in strength. Alternatively, the random orientation of the fibers may have resulted in potential weak planes through the prisms. However, an increase in the Komponent replacement level led to a higher normalized modulus of rupture for the composite prism sections. Because Komponent is a shrinkage-compensating cement, the increased replacement could have led to fewer shrinkage cracks along the bond surface, therefore increasing the overall flexural strength of the prism. Because there was no bond surface to shrink away from in the monolithic prisms, this increase was not seen. The increased modulus of rupture strength could also be attributed to the suspension of fibers within the mix. The faster slump loss of higher Komponent replacement concretes could also have led to a more random suspension of fibers within the concrete, therefore increasing the possibility that a fiber crosses any specific flexural crack.

Similar to the composite modulus of rupture tests, an increase in the Komponent replacement level led to a higher bond strength. As described earlier, this could be due to an improved bond between the control concrete and the FR-SCC repair concrete due to a reduction in shrinkage cracking. Because the

specimen failed along the bond plane, it is unlikely that the distribution of fibers within the mix played a significant role in this increased strength.

6.3.3 Full-Scale Testing

The two sets of repair beams were statistically equivalent to the control beams. They had similar ultimate moments, almost identical load versus deflection plots, and had relatively similar cracking behaviors. This is due to the high workability properties that can be offered by FR-SCC (filling and passing ability, filling capacity, and stability), its adequate durability, as well as its high mechanical and structural properties. There were a few differences, however, between the control and repaired beams. One of the primary differences was their respective cracking moments, which surprisingly decreased as Komponent replacement increased. As described in the analysis and interpretation of the small-scale results, this could be due to the existence of a shrinkage plane along the bond surface. This shrinkage plane allows for shrinkage cracks to develop as the two separate concretes cure, shrink, and try to pull away from each other.

Another slight difference was the cracking pattern along the repair line. There were a few instances where the cracks transversed horizontally a short distance before resuming their upward trend. This situation would indicate the possibility of a slight debonding or slippage between the repair material and the base concrete due to the various reasons described during the small-scale analysis.

6.4 RECOMMENDATIONS

Due to the limited number of studies into the structural behavior of FR-SCC for the repair of bridge substructures, further research is needed to make comparisons and conclusions across a larger database. To better understand the influence of a FR-SCC repair on the structural behavior of a concrete beam, additional variables important to the design must also be investigated. A list of the testable variables relating to the structural characteristics and material properties of the repaired beam is given below:

- Perform tests with a wider variation in fiber lengths to investigate its effect on crack propagation
- Perform tests with a wider variation in fiber amounts to investigate its effect on flow properties
- Perform tests with a wider variation in fiber material to investigate its effect on flow properties as well as structural performance
- Perform tests with different surface conditions to investigate its effect on the bond between the repair and the control concrete
- Perform tests with a wider variation in coarse aggregates to investigate their effect on the flow properties as well as the structural performance
- Perform tests while monitoring crack widths to investigate the effectiveness of the fibers on holding cracks closed

BIBLIOGRAPHY

ACI 318 (2014). Building Code Requirement for Structural Concrete, Farmington Hills, MI.

ASTM A 615 (2009). Standard Specification for Deformed and Plain Carbon-Steel Bars for Concrete Reinforcement. *American Society for Testing and Materials.* West Conshohocken, PA.

ASTM C 39 (2015). Standard Test Method for Compressive Strength of Cylindrical Concrete Specimens. *American Society for Testing and Materials.* West Conshohocken, PA.

ASTM C 78 (2010). Standard Test Method for Flexural Strength of Concrete (Using Simple Beam with Third-Point Loading). *American Society for Testing and Materials.* West Conshohocken, PA.

ASTM C 138 (2016). Standard Test Method for Density (Unit Weight), Yield, and Air Content (Gravimetric) of Concrete. *American Society for Testing and Materials.* West Conshohocken, PA.

ASTM C 143 (2015). Standard Test Methods for Slump of Hydraulic Cement Concrete. *American Society for Testing and Materials.* West Conshohocken, PA.

ASTM C 231 (2014). Standard Test Method for Air Content of Freshly Mixed Concrete by the Pressure Method. *American Society for Testing and Materials.* West Conshohocken, PA.

ASTM C 469 (2014). Standard Test Method for Static Modulus of Elasticity and Poisson's Ratio of Concrete in Compression. *American Society for Testing and Materials.* West Conshohocken, PA.

ASTM C 496 (2011). Standard Test Method for Splitting Tensile Strength of Cylindrical Concrete Specimens. *American Society for Testing and Materials.* West Conshohocken, PA.

ASTM C 882 (2013). Standard Test Method for Bond Strength of Epoxy-Resin Systems Used With Concrete By Slant Shear. *American Society for Testing and Materials.* West Conshohocken, PA.

ASTM C 1611 (2014). Standard Test Method for Slump Flow of Self-Consolidating Concrete. *American Society for Testing and Materials.* West Conshohocken, PA.

ASTM E 8 (2015). Standard Test Method for Tension Testing of Metallic Materials. *American Society for Testing and Materials.* West Conshohocken, PA.

Bui, Van K., Akkaya, Yilmaz, Sha, Surendra. "Rheological Model for Self-Consolidating Concrete." *Materials Journal.* Vol. 99. Issue 6. 2002. pp. 549-559.

CEB-FIP Model Code for Concrete Structures (1990). "Evaluation of the Time Dependent Behaviour of Concrete." *Bulletin d'Information*. No. 199, Comite European du Béton/Fédération international de la Precontrainte, Lausanne, 1991, pp. 201.

Cohen, Michael. "Structural Behaviour of Self Consolidating Steel Fiber Reinforced Concrete Beams." Masters Thesis, Ottawa-Carleton Institue for Civil Engineering, 2012.

Emmons, P.H. "Concrete Repair and Maintenance Illustrated." *Construction Publishers and Consultants*. 1993.

Holt, Reggie. *Self-Consolidating Concrete.* 2003. 21 January 2015. <www.fhwa.dog.gov/hfl>.

Kassimi, Fodhil. "Development and Performance of Fiber-Reinforced Self-Consolidating Concrete for Repair Applications." PhD dissertation, University of Sherbrooke, 2013.

Kassimi, Fodhil, El-Sayed, Ahmend K., Khayat, Kamal. "Performance of Fiber-Reinforced Self-Consolidating Concrete for Repair of Reinforced Concrete Beams." *ACI Structural Journal.* 2014. pp. 1277-1286.

Khayat, K. H., Ghezal, A., Hadriche. "Utility of Statistical Models in Proportioning Self-Consolidating Concrete." *Materials and Structures.* 33rd Edition. 1999a. pp. 338-344.

Khayat, Kamal. "Workability, Testing, and Performance of Self-Consolidating Concrete." *Materials Journal.* Vol. 96. Issue 3. 1999b. pp. 346-353.

USDOT. "Deficient Bridges by State and Highway System 2013," *Bridges and Structures."* U.S. Department of Transportation Federal Highway Administration. 7 April 2014. 17 Novemeber 2014. <www.fhwa.dot.gov/bridge>.

APPENDIX A. FIBER DATA SHEET

BASF
We create chemistry

3

03 30 00	Cast-In-Place Concrete
03 37 13	Shotcrete
03 40 00	Precast Concrete
03 70 00	Mass Concrete

MasterFiber® MAC Matrix

Macrosynthetic Fiber

Description

MasterFiber MAC Matrix product is a macrosynthetic fiber that is manufactured from a proprietary blend of polypropylene resins, and meets the requirements of ASTM C 1116/C 1116M "Standard Specification for Fiber-Reinforced Concrete."

MasterFiber MAC Matrix product also meets the requirements of CSA B66-10 "Design, material, and manufacturing requirements for prefabricated septic tanks and sewage holding tanks."

Applications

Recommended for use in:

- Shotcrete
- Composite metal decks
- Industrial and warehouse floors
- Pavements
- Precast concrete
- Residential and commercial slabs-on-ground
- Thin-wall precast
- Tunnel linings
- Wall systems
- Whitetopping/overlays

Features

MasterFiber MAC Matrix product is engineered for use as secondary reinforcement to control shrinkage and temperature cracking, and settlement cracking.

MasterFiber MAC Matrix product was created specifically to replace welded-wire reinforcement and No. 3 and No. 4 (10 mm and 13 mm) reinforcing bars that are typically used as temperature and shrinkage reinforcement.

MasterFiber MAC Matrix product has the following features:

- Excellent flexural performance
- Excellent finishability

Benefits

- Eliminates the need for welded-wire reinforcement (WWR) and small diameter bars used as secondary reinforcement, depending on the application
- Effective tight crack control
- Provides excellent control of settlement cracking
- Improves green strengths and permits earlier stripping of forms with less rejection
- Reduces construction time and overall labor and material costs
- Reduces the effects of handling and transportation stresses
- Increases flexural toughness, impact and shatter resistance

MASTER® BUILDERS SOLUTIONS

Performance Characteristics

Physical Properties	
Specific Gravity	0.91
Melting Point	320 °F (160 °C)
Ignition Point	1094 °F (590 °C)
Absorption	Nil
Alkali Resistance	Excellent
Tensile Strength	85 ksi (585 MPa)
Length	2.1 in. (54 mm)
Aspect Ratio	67
Fiber Type	Embossed
Material	100% virgin polypropylene
Chemical Resistance	Excellent

Guidelines for Use

Dosage: The dosage range of MasterFiber MAC Matrix product is 3 to 12 lb/yd³ (1.8 to 7.2 kg/m³). The recommended dosage range for slab-on-ground applications is typically 3 to 5 lb/yd³ (1.8 to 3 kg/m³). For shotcrete, the typical dosage range of MasterFiber MAC Matrix product is 8 to 12 lb/yd³ (4.8 to 7.2 kg/m³).

Mixing: MasterFiber MAC Matrix product should be introduced at the beginning of the mixing cycle, but not at the same time as the cement. For slab-on-ground applications, the entire bag should be dispensed into the mixer to allow for easy handling, while leaving no waste on site. For shotcrete, the bag should be opened so that the fibers can be dispensed directly into the mixer. Three to five minutes of additional mixing will be required to disperse the fibers depending on when the product is added to the mixer. BASF recommends utilizing good concrete mixing practices as outlined in ASTM C 1116/C 1116M.

Engineering Specifications

MasterFiber MAC Matrix product is an option for the replacement of WWR and is an easy-to-use secondary reinforcing system that is rust proof, alkali resistant, and compliant with industry codes when mixed in accordance with ASTM C 1116/C 1116M. MasterFiber MAC Matrix product enhances safety and should be specified for use in applications for:

- Increased flexural toughness
- Reduced rebound
- Increased cohesion
- Increased impact and shatter resistance
- Extended pump life
- Replacement of WWR and other secondary reinforcement
- Improved residual strength
- Improved durability
- Use in areas requiring no metal

MasterFiber MAC Matrix product also conforms to the requirements of CSA B66-10 "Design, material, and manufacturing requirements for prefabricated septic tanks and sewage holding tanks".

Product Notes

MasterFiber MAC Matrix product is not a replacement for primary/structural steel reinforcement and should not be used to replace reinforcing steel where the area of the steel is used in the calculation of the load-carrying capacity of the concrete member.

Placement and Finishing: BASF recommends that the standard practices detailed in ACI 302.1R, ACI 506.1R and ACI 544.3R for placing, finishing and curing concrete be followed when using MasterFiber MAC Matrix product.

Storage and Handling

MasterFiber MAC Matrix product should be stored in a clean, dry area protected from the weather and at temperatures below 140 °F (60 °C). Avoid storing near strong oxidizers and avoid sources of ignition. Use caution when stacking to avoid unstable conditions. Store in a sprinkled warehouse.

Packaging

MasterFiber MAC Matrix product is packaged in a 5 lb (2.3 kg) degradable bag that can be added directly to the mixing system. For shotcrete, the fibers are packaged in 11 lb (5 kg) and 15.4 lb (7 kg) bags which should be opened prior to dispensing the fibers into the mixer.

Related Documents

Safety Data Sheets: MasterFiber MAC Matrix

Additional Information

For additional information on MasterFiber MAC Matrix product, contact your local sales representative

The Admixture Systems business of BASF's Construction Chemicals division is the leading provider of solutions that improve placement, pumping, finishing, appearance and performance characteristics of specialty concrete used in the ready-mixed, precast, manufactured concrete products, underground construction and paving markets. For over 100 years we have offered reliable products and innovative technologies, and through the Master Builders Solutions brand, we are connected globally with experts from many fields to provide sustainable solutions for the construction industry.

Limited Warranty Notice

BASF warrants this product to be free from manufacturing defects and to meet the technical properties on the current Technical Data Guide, if used as directed within shelf life. Satisfactory results depend not only on quality products but also upon many factors beyond our control. BASF MAKES NO OTHER WARRANTY OR GUARANTEE, EXPRESS OR IMPLIED, INCLUDING WARRANTIES OF MERCHANTABILITY OR FITNESS FOR A PARTICULAR PURPOSE WITH RESPECT TO ITS PRODUCTS. The sole and exclusive remedy of Purchaser for any claim concerning this product, including but not limited to, claims alleging breach of warranty, negligence, strict liability or otherwise, is shipment to purchaser of product equal to the amount of product that fails to meet this warranty or refund of the original purchase price of product that fails to meet this warranty, at the sole option of BASF. Any claims concerning this product must be received in writing within one (1) year from the date of shipment and any claims not presented within that period are waived by Purchaser. BASF WILL NOT BE RESPONSIBLE FOR ANY SPECIAL, INCIDENTAL, CONSEQUENTIAL (INCLUDING LOST PROFITS) OR PUNITIVE DAMAGES OF ANY KIND.

Purchaser must determine the suitability of the products for the intended use and assumes all risks and liabilities in connection therewith. This information and all further technical advice are based on BASF's present knowledge and experience. However, BASF assumes no liability for providing such information and advice including the extent to which such information and advice may relate to existing third party intellectual property rights, especially patent rights, nor shall any legal relationship be created by or arise from the provision of such information and advice. BASF reserves the right to make any changes according to technological progress or further developments. The Purchaser of the Product(s) must test the product(s) for suitability for the intended application and purpose before proceeding with a full application of the product(s). Performance of the product described herein should be verified by testing and carried out by qualified experts.

MasterFiber MAC Matrix fiber, as marketed by BASF Corporation, is classified by Underwriters Laboratories Inc. for use in the following fire rated assemblies: UL D700, D800 and D900 Series Designs. Fibers to be added to the concrete mix at a maximum rate of 5.0 lb of fiber for each cubic yard (3.0 kg/m³) of concrete.

BASF Corporation
Admixture Systems
www.master-builders-solutions.basf.us

United States
23700 Chagrin Boulevard
Cleveland, Ohio 44122-5544
Tel: 800 628-9990 • Fax: 216 839-8821

Canada
1800 Clark Boulevard
Brampton, Ontario L6T 4M7
Tel: 800 387-5862 • Fax: 905 792-0651

APPENDIX B. STRUCTURAL PERFORMANCE DATA

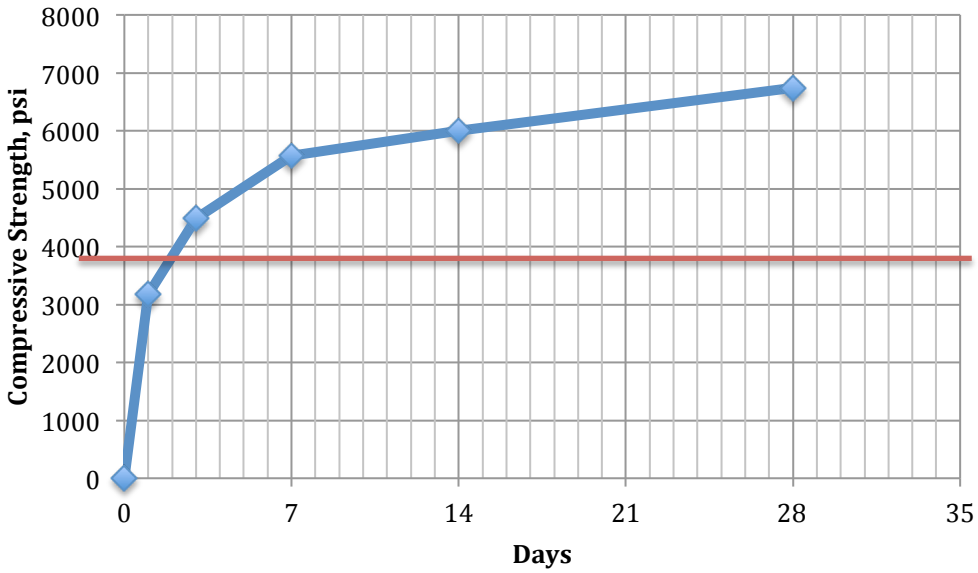

Figure B.1a C-C Compressive Strengths

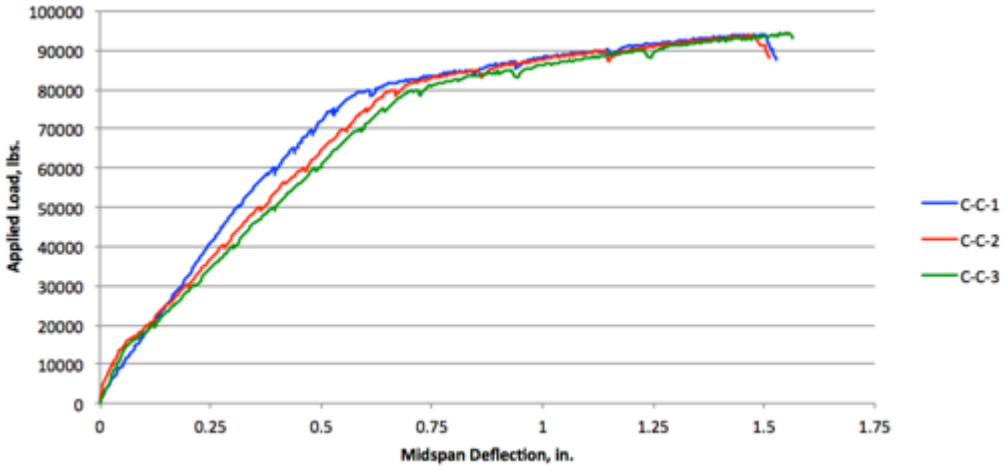

Figure B.1b C-C Midspan Deflection

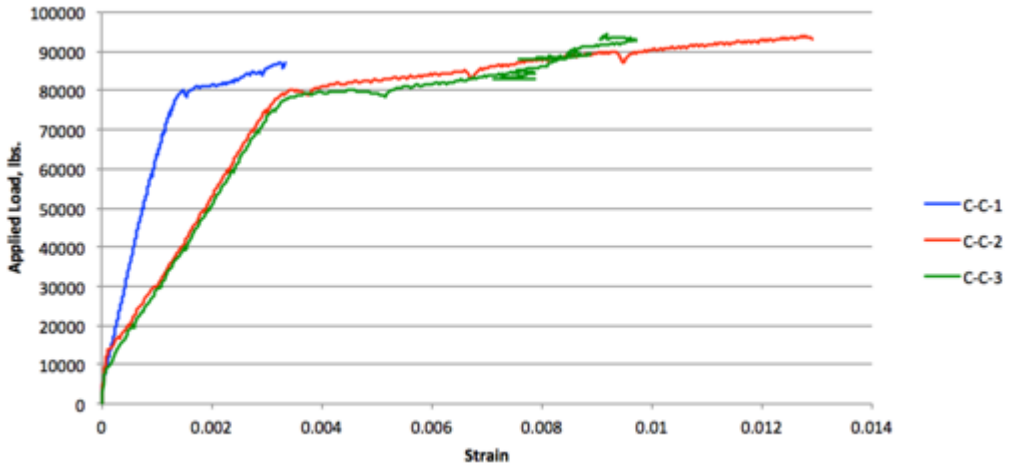

Figure B.1c C-C Steel Strain

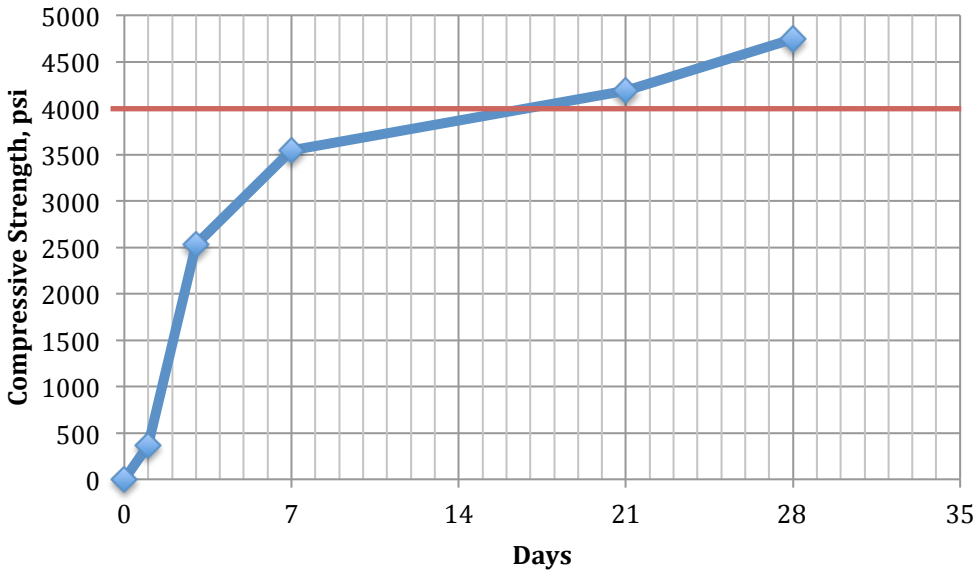

Figure B.2a C-10% Compressive Strengths

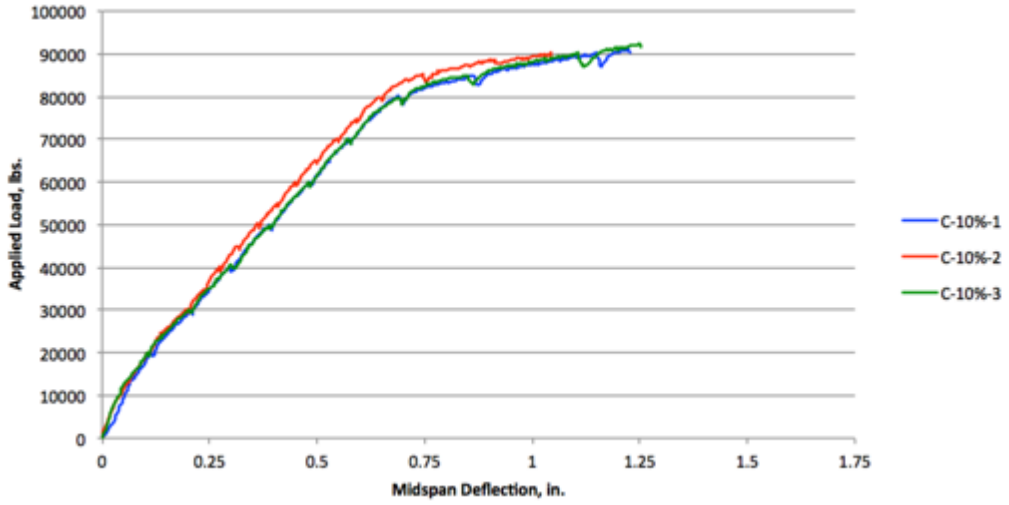

Figure B.2b C-10% Midspan Deflection

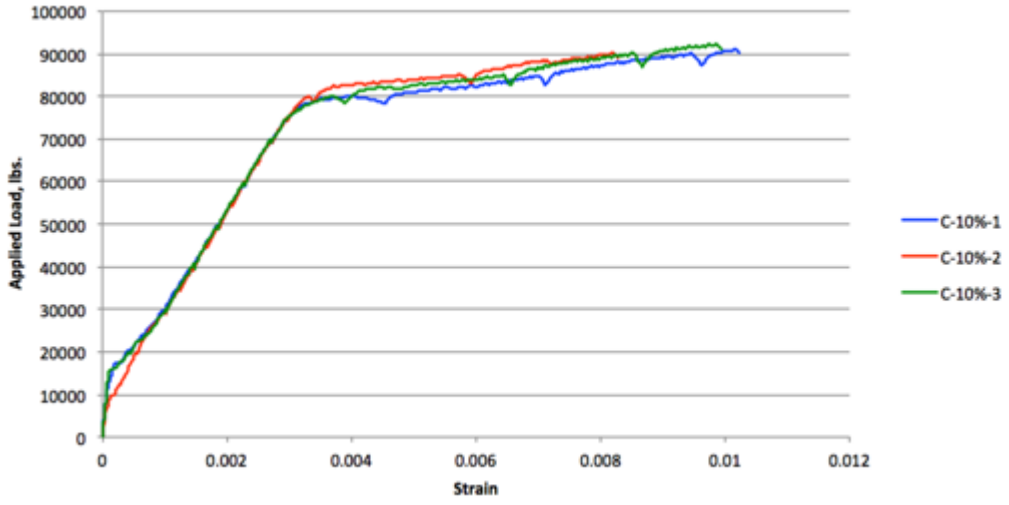

Figure B.2c C-10% Steel Strain

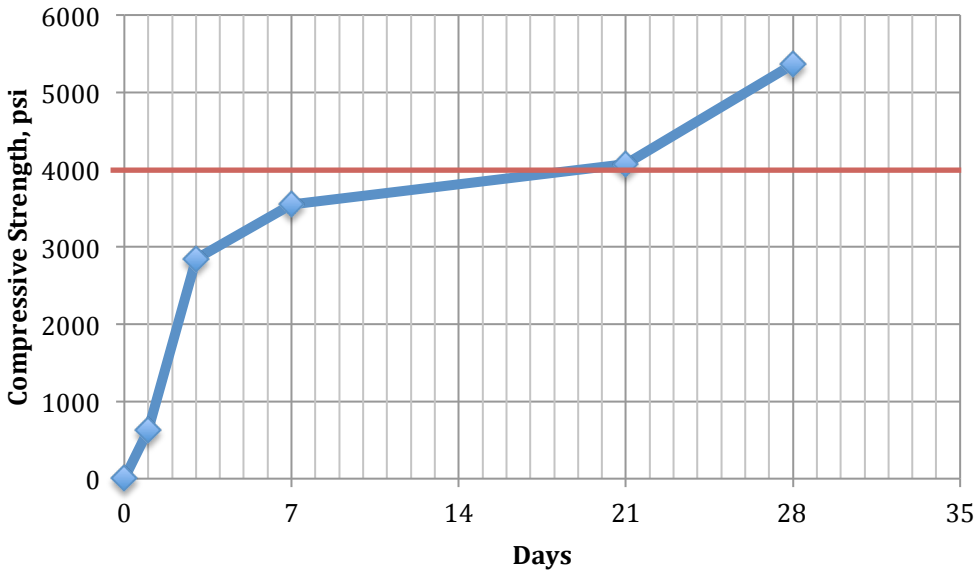

Figure B.3a C-15% Compressive Strengths

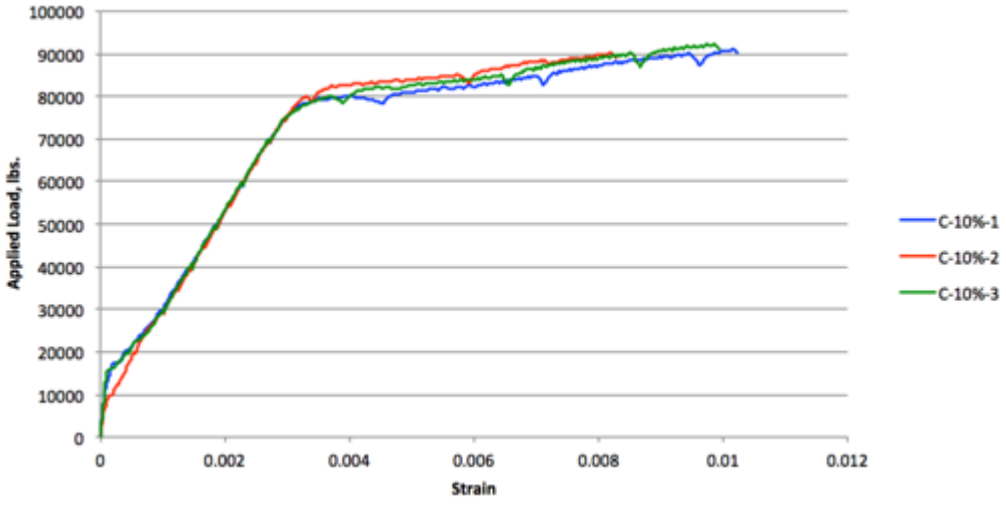

Figure B.3b C-15% Midspan Deflection

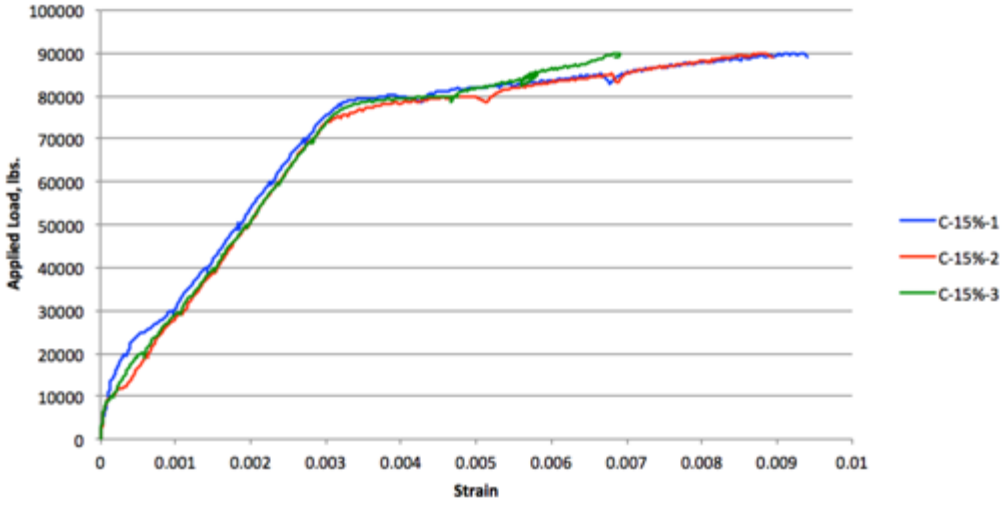

Figure B.3c C-15% Steel Strain

APPENDIX C. PHOTOGRAPHS OF FULL-SCALE TESTS

Figure C.1a C-C-1 Set-Up

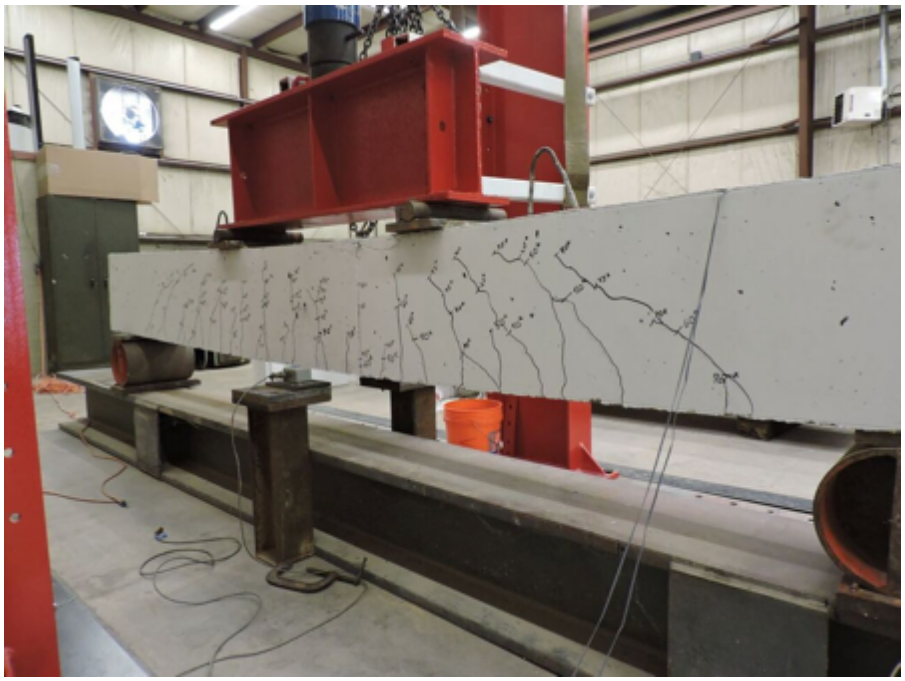

Figure C.1b C-C-1 at Failure

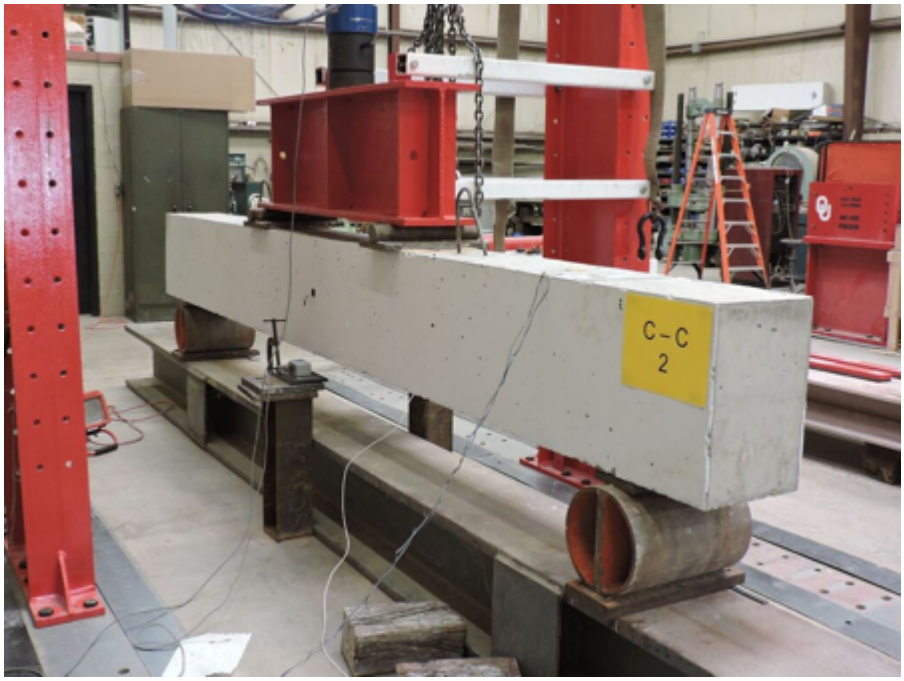

Figure C.2a C-C-2 Set-Up

Figure C.2b C-C-2 at Failure

Figure C.3a C-C-3 Set-Up

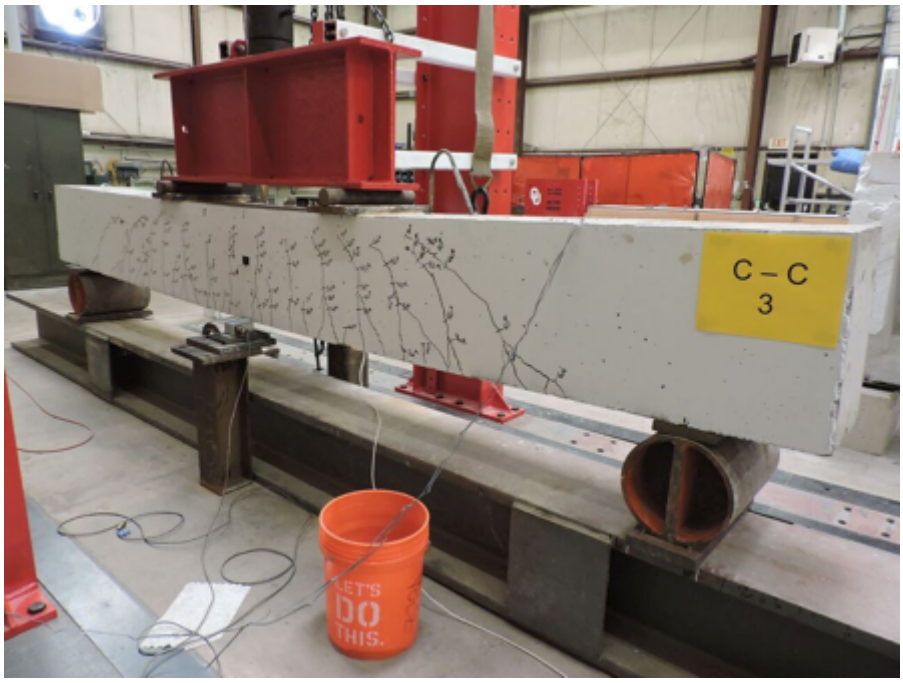

Figure C.3b C-C-3 at Failure

Figure C.4a C-10%-1 Set-Up

Figure C.4b C-10%-1 at Failure

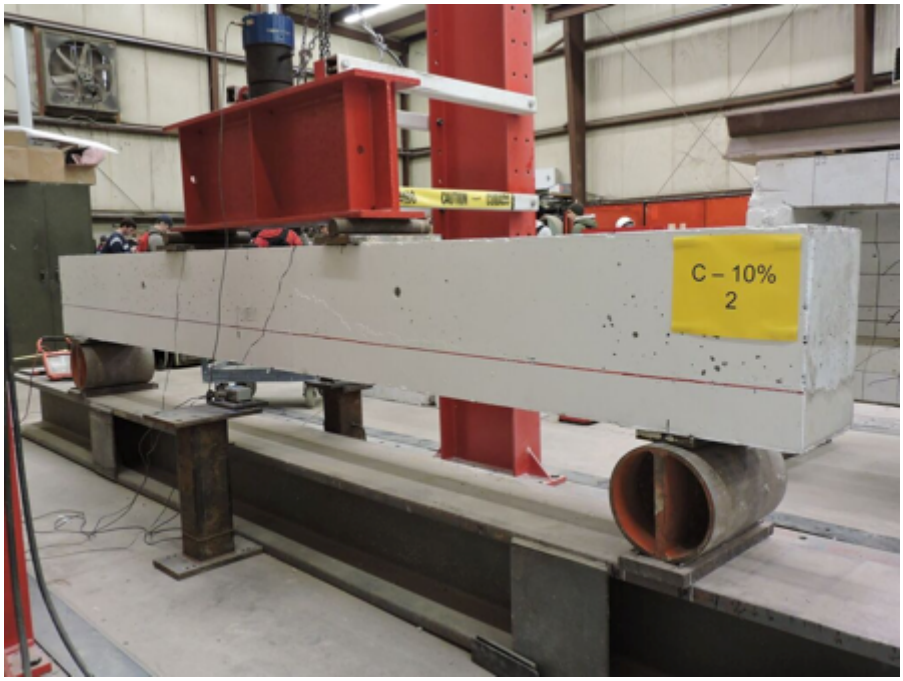

Figure C.5a C-10%-2 Set-Up

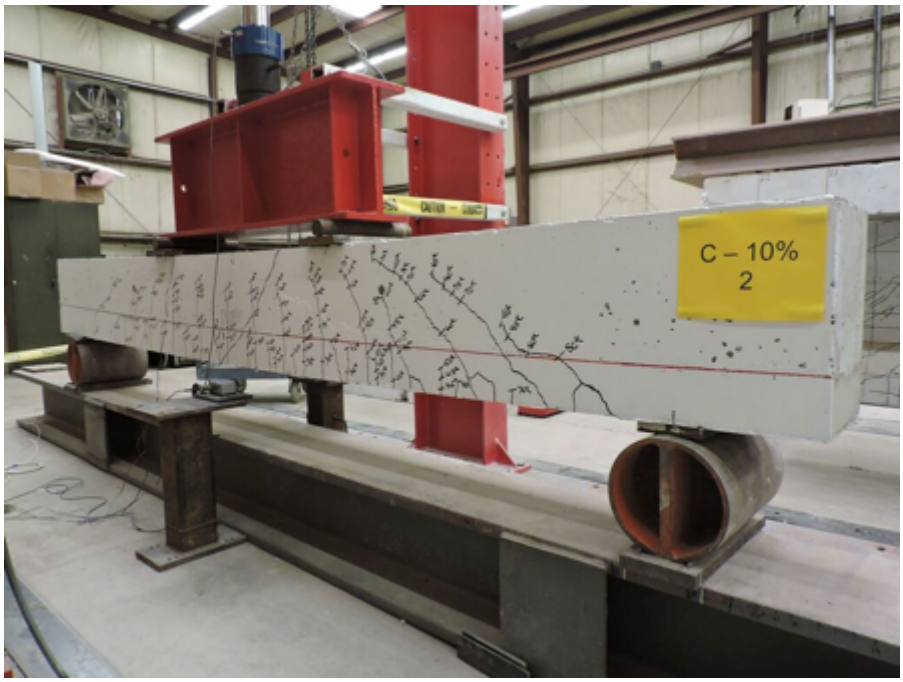

Figure C.5b C-10%-2 at Failure

Figure C.6a C-10%-3 Set-Up

Figure C.6b C-10%-3 at Failure

Figure C.7a C-15%-1 Set-Up

Figure C.7b C-15%-1 at Failure

Figure C.8a C-15%-2 Set-Up

Figure C.8b C-15%-2 at Failure

Figure C.9a C-15%-3 Set-Up

Figure C.9b C-15%-3 at Failure